NASA TECHNICAL NOTE

NASA TN D-8096

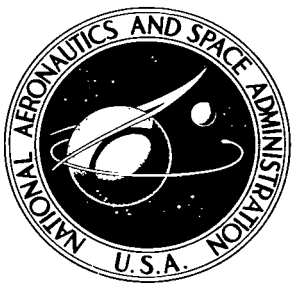

NASA TN D-8096
c. 1

ANALYSIS OF LIQUID-METAL-JET IMPINGEMENT COOLING IN A CORNER REGION AND FOR A ROW OF JETS

Robert Siegel

Lewis Research Center
Cleveland, Ohio 44135

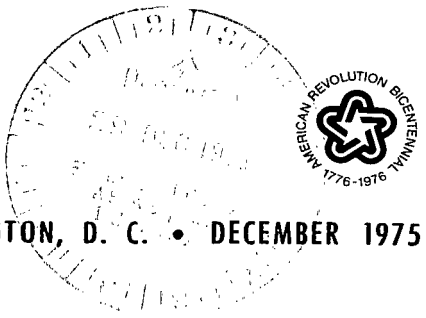

NATIONAL AERONAUTICS AND SPACE ADMINISTRATION • WASHINGTON, D. C. • DECEMBER 1975

1. Report No.	2. Government Accession No.	3. Recip
NASA TN D-8096		

4. Title and Subtitle	5. Report Date
ANALYSIS OF LIQUID-METAL-JET IMPINGEMENT COOLING IN A CORNER REGION AND FOR A ROW OF JETS	December 1975
	6. Performing Organization Code

7. Author(s)	8. Performing Organization Report No.
Robert Siegel	E-8325
	10. Work Unit No.
9. Performing Organization Name and Address	505-04
Lewis Research Center National Aeronautics and Space Administration Cleveland, Ohio 44135	11. Contract or Grant No.
	13. Type of Report and Period Covered
12. Sponsoring Agency Name and Address	Technical Note
National Aeronautics and Space Administration Washington, D.C. 20546	14. Sponsoring Agency Code

15. Supplementary Notes

16. Abstract

A conformal mapping method is used to analyze liquid-metal-jet impingement heat transfer. The jet flow region and energy equation are transformed to correspond to uniform flow in a parallel plate channel with nonuniform heat addition along a portion of one wall. The exact solution for the wall-temperature distribution is obtained in the transformed channel, and the results are then mapped back into the physical plane. Two geometries are analyzed. One is for a single slot jet directed either into an interior corner formed by two flat plates, or over the external sides of the corner. The flat plates are uniformly heated, and the corner can have various included angles. The heat-transfer coefficient at the stagnation point at the apex of the plates is obtained as a function of the corner angle, and temperature distributions are calculated along the heated walls. The second geometry is an infinite row of uniformly spaced parallel slot jets impinging normally against a uniformly heated plate. The heat-transfer behavior is obtained as a function of the spacing between the jets. Results are given for several jet Péclet numbers from 5 to 50.

17. Key Words (Suggested by Author(s))	18. Distribution Statement
Conformal mapping; Corner flow; Impingement heat transfer; Jet heat transfer; Liquid-metal heat transfer; Liquid-metal jet	Unclassified - unlimited STAR category 34 (rev.)

19. Security Classif. (of this report)	20. Security Classif. (of this page)	21. No. of Pages	22. Price*
Unclassified	Unclassified	53	$4.25

* For sale by the National Technical Information Service, Springfield, Virginia 22161

ANALYSIS OF LIQUID-METAL-JET IMPINGEMENT COOLING IN A CORNER REGION AND FOR A ROW OF JETS

by Robert Siegel

Lewis Research Center

SUMMARY

Jet impingement is a possible means for providing effective localized heat transfer. Two configurations are analyzed here for jet impingement against uniformly heated surfaces. The first is for flow into the interior or over the exterior of a corner formed at the apex of two flat plates. The second is for an infinite row of parallel slot jets impinging normally against a plate. Liquid metals are very effective heat-transfer fluids and are specifically studied here as a possible means for obtaining high heat-transfer coefficients. An analytical aid in the study of liquid-metal heat transfer is the fact that the Prandtl number is small, and hence viscous diffusion effects are small compared with the molecular diffusion of heat. To a good approximation the flow can then be assumed inviscid with regard to the solution of the energy equation. For inviscid flow the jet region can be analyzed by conformal mapping. The flow region is transformed into a region of uniform flow between parallel plates. The energy equation is also transformed into the coordinates of the parallel plate region and takes the form of an equation for which the exact solution is known. The solution is then transformed back into the physical plane to obtain the local heat-transfer characteristics along the impingement surfaces. The heat-transfer behavior is given for incident jet Péclet numbers from 5 to 50. The results show how the heat transfer improves as the included corner angle or the jet spacing is increased.

INTRODUCTION

Jet impingement is a possible means for obtaining effective localized cooling. The specific type of fluid considered here is a liquid metal, which is a very effective heat-transfer medium that can be used at high temperatures without requiring high pressures. In this report some effects of impingement plate and jet geometry are investigated by analyzing the heat transfer for impinging slot jets in two configurations. One of these is the somewhat confined flow geometry of a single slot jet impinging in a corner region

formed by two flat plates joined at an angle to each other. The heat-transfer behavior is obtained as a function of corner angle. Since the same solution applies for both flow into the interior of the corner and over the exterior of the corner, results were computed for a wide range of corner angles ($\delta = 60^{\circ}$ to 360°). The second geometry considered is an infinite row of uniformly spaced parallel slot jets impinging against a flat plate. It is desired to obtain the heat-transfer dependence on the spacing between the jets. This geometry was studied for air in reference 1.

The present work is an extension of reference 2 where the impingement heat transfer was obtained for a single jet flowing normally against a flat plate. The solution in reference 2 is a limiting case for both geometries treated here; for the corner flow it corresponds to an included angle δ of 180°, while for the row of parallel jets it corresponds to infinite spacing between the jets. The theory is based on the use of conformal mapping, which is valid for inviscid flow; hence, the theory utilizes a potential flow approximation with regard to the fluid behavior. Inviscid flow is a good approximation for liquid metals for the jet Péclet number range treated here ($Pe \leq 50$). These fluids have very small Prandtl numbers ($Pr \approx 0.005$ to 0.02). Because the Prandtl number is the ratio of viscous to thermal diffusivity, for a situation where both the viscous and thermal boundary layers are developing simultaneously, the viscous layer will be very thin compared with the thermal layer thickness. The heat transfer can thus be computed quite well by neglecting the viscous boundary layer and using an inviscid approximation with regard to the flow.

The free streamlines bounding the jet, and the fluid velocity along the heated boundary (this velocity is needed to evaluate the solution of the energy equation) are obtained by mapping the jet region into a potential plane. In this plane the flow geometry becomes a strip of constant width. The mapping is achieved by use of an intermediate hodograph (complex velocity) plane.

The strip region into which the jet maps in the potential plane is a convenient region in which to solve the energy equation. When the energy equation is transformed into the coordinates of the potential plane, it has the same form as the energy equation for a uniform velocity in a parallel plate channel. The boundary condition of uniform heating at the impingement plate transforms into a nonuniform heating condition along one of the channel boundaries. The analytical solution is available for this situation, so the solution is obtained in the potential plane and then mapped back into the physical geometry. This yields the temperature distribution along the uniformly heated wall. The heat transfer performance at the stagnation point is also expressed as a heat-transfer coefficient, and its behavior is compared with that for single-jet flat-plate impingement. This clearly shows the effect of corner angle and spacing between jets in an infinite row.

ANALYSIS

Description of Physical Situation

The flow configurations, which are two-dimensional, are shown in figures 1 and 2. (See appendix A for symbol definitions.) In figure 1 a slot jet having a half-width b impinges against a wedge-shaped plate either into the corner or over the outside of the corner, the special intermediate case being impingement against a flat plate. The plates forming the corner have a uniform heat flux q_w supplied along them. There is a stagnation point where the centerline of the jet meets the apex of the corner, and it is the heat-transfer behavior in this region that is of most interest. The impingement plate is assumed to extend to infinity in the direction of the flow along it, but any plate length that is longer than several jet widths would provide the same flow pattern in the stagnation region. The nozzle forming the jet is far enough from the plate so that the impingement does not alter the uniform flow leaving the nozzle. For impingement of a single jet against a flat plate, this is true for nozzles more than about three jet widths away from the surface. After turning, the flow moves out along each half of the plate, and, for the condition of inviscid-irrotational flow considered here, the flow becomes parallel to the plate with an asymptotic thickness b.

In figure 2 the geometry is shown for an infinite row of parallel slot jets striking a uniformly heated wall. The half width of the incoming jets is b, and there is a uniform half spacing S between them.

Flow Characteristics of Jet

The fluid being considered here is a liquid metal, and hence it has a very low Prandtl number ($Pr \approx 0.005$ to 0.02). The Prandtl number is the ratio of the fluid viscous diffusivity to the molecular diffusivity of heat. In a boundary-layer type of flow over a heated surface where both the viscous and thermal boundary layers are developing simultaneously, the viscous layer in a liquid metal will be very thin compared with the thermal layer thickness and can be neglected. A flow that is initially irrotational, as is the case for the approaching jet, will develop little vorticity and can be assumed to remain irrotational. Consequently, the jet configuration can be obtained from free streamline theory by use of conformal mapping. The details of the mappings are given in appendixes B and C, and only the final results are summarized here.

Corner flow. - Because of symmetry, only half of the jet need be considered. It is shown with some additional notation in figure 3(a) and in dimensionless form in figure 3(b). In the mapping the flow region is transformed from the dimensionless physical plane into a potential plane in which the free streamline $\widehat{12}$ and the streamline $\widehat{345}$ along

the jet centerline and the heated plate become parallel lines (fig. 4). Thus in the potential plane the flow region is a parallel plate channel where heating is being applied to a portion of one side. As will be given later, the energy equation is solved in this channel flow region, and to transform the calculated plate temperatures from the potential plane to the physical plane the relation is needed between Φ in figure 4 and L in figure 3(b). This relation is obtained from the mapping in appendix B as

$$L = \frac{8}{\pi} \int_0^{\xi} \frac{d\xi}{\xi^{\beta}(1 - \xi^4)} \qquad 0 \le \xi \le 1 \tag{1a}$$

$$\Phi = \frac{4}{\pi} \tanh^{-1}(\xi^2) \qquad 0 \le \xi \le 1 \tag{1b}$$

To obtain an indication of the flow pattern, the free streamlines were calculated. The coordinates are given by

$$X = X_o - \frac{4}{\pi} \int_{\pi/4}^{\theta} \frac{\cos\left[\theta(1 + \beta) - \beta\frac{\pi}{2}\right]}{\sin 2\theta} d\theta \qquad 0 \le \theta \le \frac{\pi}{2} \tag{2a}$$

$$Y = Y_o + \frac{4}{\pi} \int_{\pi/4}^{\theta} \frac{\sin\left[\theta(1 + \beta) - \beta\frac{\pi}{2}\right]}{\sin 2\theta} d\theta \qquad 0 \le \theta \le \frac{\pi}{2} \tag{2b}$$

The X_o and Y_o are given by (these are the X and Y at $\theta = \pi/4$)

$$X_o = \frac{8}{\pi} \cos\left[\frac{\pi}{4}(1 + \beta)\right] F(\beta) \tag{3a}$$

$$Y_o = \frac{8}{\pi} \sin\left[\frac{\pi}{4}(1 + \beta)\right] F(\beta) \tag{3b}$$

where

$$F(\beta) = \int_0^1 \frac{d\eta}{\eta^{\beta}(1 + \eta^4)}$$

Row of jets. - From symmetry it is only necessary to consider the region between the centerlines of a jet and an adjacent backflow region (fig. 5). In the potential plane this region maps into a strip in the same fashion as the corner flow discussed previously. The heated wall $\widehat{71}$ occupies a portion of the zero streamline. The mapping between figures 5 and 6 is given in appendix C and is in terms of elliptic functions. The relation between X and Φ along the heated wall is

$$X = \frac{2}{\pi}\left[\tan^{-1}\left(\frac{k' \operatorname{sn} \xi}{\operatorname{cn} \xi}\right) + \xi\right] \qquad -\frac{S}{2b} \le X \le \frac{S}{2b} \tag{4a}$$

and

$$\Phi = \frac{1}{\pi} \ln\left[\frac{(1 + k)\operatorname{sn} \xi}{(1 - k)\operatorname{sn} \xi}\right] \qquad -\frac{1}{\pi}\ln\left(\frac{1 + k}{1 - k}\right) \le \Phi \le \frac{1}{\pi}\ln\left(\frac{1 + k}{1 - k}\right) \tag{4b}$$

where

$$-K \le \xi \le K$$

To obtain k and k', the K is first obtained from the jet spacing using the relation

$$K = \frac{\pi}{2}\left(\frac{S}{2b} - 1\right) \qquad \frac{\pi}{2} \le K \le \infty \tag{5}$$

The k is then found from K by using the complete elliptic integral

$$K = \int_0^{\pi/2} \frac{d\varphi}{\sqrt{1 - k^2 \sin^2 \varphi}} \qquad 0 \le k^2 \le 1 \tag{6}$$

and k' is related to k by

$$k' = \sqrt{1 - k^2} \tag{7}$$

The coordinates of the free streamlines are given by

$$X = \frac{2}{\pi}\xi \qquad -K \leq \xi \leq K \tag{8a}$$

and

$$Y = \frac{2}{\pi}\left[K' + \frac{1}{2}\ln\left(\frac{dn\ \xi + k'}{dn\ \xi - k'}\right)\right] \qquad -K \leq \xi \leq K \tag{8b}$$

where

$$K' = K(k') = \int_0^{\pi/2} \frac{d\varphi}{\sqrt{1 - k'^2 \sin^2 \varphi}}$$

The Governing Energy Equation and Boundary Conditions

The energy equation in the two-dimensional flow region is given as a balance of convection and conduction by

$$\rho C_p \vec{u} \cdot \nabla t = \kappa \nabla^2 t \tag{9}$$

For inviscid-irrotational flow the fluid velocity can be expressed as the gradient of a potential φ:

$$\vec{u} = \nabla \varphi \tag{10}$$

where φ satisfies Laplace's equation

$$\nabla^2 \varphi = 0 \tag{11}$$

The velocity components are related to the stream function by the Cauchy-Riemann equations:

$$u = \frac{\partial \varphi}{\partial x} = \frac{\partial \psi}{\partial y} \tag{12a}$$

and

$$v = \frac{\partial \varphi}{\partial y} = - \frac{\partial \psi}{\partial x} \tag{12b}$$

By use of equation (10) the energy equation then becomes

$$\rho C_p \nabla \varphi \cdot \nabla t = \kappa \nabla^2 t \tag{13}$$

The thermal boundary conditions are as follows (the boundaries without parentheses correspond to fig. 3(b) while those in parentheses correspond to fig. 5). Along the cross section of the incoming undisturbed jet, the fluid is at a uniform temperature t_∞;

$$t = t_\infty \qquad x, y \text{ on } \widehat{23}\ (\widehat{56}) \tag{14}$$

It is assumed that along the free streamline there is little heat loss in comparison with the convective heat flow within the jet, so this boundary is assumed insulated:

$$\hat{n}_s \cdot \nabla t = 0 \qquad x, y \text{ on } \widehat{12}\ (\widehat{345}) \tag{15}$$

Boundaries formed by symmetry lines have no heat flow across them and hence also act as insulated boundaries:

$$\frac{\partial t}{\partial x} = 0 \qquad x, y \text{ on } \widehat{34}\ (\widehat{12} \text{ and } \widehat{67}) \tag{16}$$

Along the solid boundary a uniform heat flux q_w is imposed so that

$$\frac{\partial t}{\partial n_w} = - \frac{q_w}{\kappa} \qquad x, y \text{ on } \widehat{45}\ (\widehat{71}) \tag{17}$$

Before obtaining the solution, the energy equation and boundary conditions are placed in dimensionless form. Using the dimensionless variables defined in appendix A the energy equation becomes

$$\frac{Pe}{2} \tilde{\nabla} \Phi \cdot \tilde{\nabla} T = \tilde{\nabla}^2 T \tag{18}$$

with the boundary conditions

$$\hat{n}_s \cdot \tilde{\nabla} T = 0 \qquad x, y \text{ on } \widehat{12}\ \widehat{(345)} \tag{19}$$

$$\frac{\partial T}{\partial X} = 0 \qquad x, y \text{ on } \widehat{34}\ (\widehat{12} \text{ and } \widehat{67}) \tag{20}$$

$$\frac{\partial T}{\partial N_w} = -1 \qquad x, y \text{ on } \widehat{45}\ \widehat{(71)} \tag{21}$$

The strip regions in figures 4 and 6 have a simple geometry and hence are convenient regions in which to solve the energy equation. Since in the potential plane streamlines with equal numerical increments are spaced equal distances apart, the strip represents a channel having a uniform velocity distribution across its width. The energy equation (eq. (18)) has the same form as that of equation (16) of reference 3, where it is shown how the equation can be transformed from the dimensionless X, Y plane to the Φ, Ψ coordinates. Using equation (26) of reference 3 yields the energy equation as

$$\frac{Pe}{2} \frac{\partial T}{\partial \Phi} = \frac{\partial^2 T}{\partial \Phi^2} + \frac{\partial^2 T}{\partial \Psi^2} \tag{22}$$

This is the same as the energy equation that applies for forced convection in a uniform velocity flow in a channel between parallel plates. The flow is in the Φ direction, and the channel width extends across the Ψ direction. If the solution is obtained in the potential plane, it can then be mapped into the physical plane since the Φ, Ψ plane is related to the X, Y plane by conformal mapping. To solve equation (22), the boundary conditions in the physical plane must be transformed into the Φ, Ψ coordinate system.

The free streamline along which equation (19) applies is a line of constant Ψ, and the normal direction to Ψ would thus be along a constant Φ line. Hence, the boundary condition in equation (19) becomes

$$\frac{\partial T}{\partial \Psi} = 0 \qquad \Phi, \Psi \text{ on } \widehat{12}\ \widehat{(345)} \tag{23}$$

The symmetry condition in equation (20) is preserved under the transformation to the potential plane. This boundary condition then becomes

$$\frac{\partial T}{\partial \Psi} = 0 \qquad \Phi, \Psi \text{ on } \widehat{34}\ (\widehat{12} \text{ and } \widehat{67}) \tag{24}$$

To transform equation (21), the fact that the normal coordinate N_w is a function of Φ and Ψ is used to yield

$$\frac{\partial T}{\partial N_w} = \frac{\partial T}{\partial \Psi}\frac{\partial \Psi}{\partial N_w} + \frac{\partial T}{\partial \Phi}\frac{\partial \Phi}{\partial N_w}$$

Since the derivative of Φ in a direction is the velocity in that direction, the $\partial\Phi/\partial N_w$ at the wall would be zero as there is no velocity normal to the wall at the wall. Then along $\widehat{45}$ using equation (21)

$$-1 = \frac{\partial T}{\partial \Psi}\frac{\partial \Psi}{\partial N_w}\bigg|_w$$

If L and N_w form a coordinate system tangential and normal to the wall, the Cauchy-Riemann equations yield

$$\frac{\partial \Psi}{\partial N_w} = \frac{\partial \Phi}{\partial L} = U_L$$

where U_L is the tangential velocity along the wall. The boundary condition then becomes

$$\frac{\partial T}{\partial \Psi} = -\frac{1}{U_L} \qquad \Phi, \Psi \text{ on } \widehat{45}\ (\widehat{71}) \tag{25}$$

From the solutions in appendixes B and C the U_L for the two geometries are given by

$$U_L(\Phi) = \left[\tanh\left(\frac{\pi\Phi}{4}\right)\right]^{(1+\beta)/2} \qquad \Phi \text{ on } \widehat{45} \text{ in figure 4} \tag{26}$$

$$U_L(\Phi) = \frac{\left[k^2 - \tanh^2\left(\frac{\pi\Phi}{2}\right)\right]^{1/2}}{k' + \left[1 - \tanh^2\left(\frac{\pi\Phi}{2}\right)\right]^{1/2}} \qquad \Phi \text{ on } \widehat{71} \text{ in figure 6} \tag{27}$$

The jet approaching the heated plate is at a uniform temperature, so in the transformed plane

$$T = T_\infty \qquad \Phi, \Psi \text{ on } \widehat{23}\ (\widehat{65}) \tag{28}$$

Solution for Wall Temperature

Considering the situation in the potential plane, the term on the left side of equation (22) represents convection along the axial (that is, Φ) direction in figures 4 and 6, and the terms on the right side are axial and transverse heat conduction. In figures 4 and 6 the geometry is a moving slab between parallel plates. The slab is at uniform temperature for large negative Φ, and the parallel planes are insulated except for a nonuniform heat addition along the positive Φ-axis in figure 4 and along a portion of the Φ-axis in figure 6. The solution for this situation including axial heat conduction was given in reference 2. The specific quantity of interest is the temperature along the wall $\widehat{45}$ in figure 3 or $\widehat{71}$ in figure 5, and this is given by

$$T_w(\Phi) - T_\infty = \frac{2}{Pe}\left[\int_{\eta_1}^{\Phi} \frac{d\eta}{U_L(\eta)} + \int_{\Phi}^{\eta_2} \frac{\exp\left[-\frac{Pe}{2}(\eta - \Phi)\right]}{U_L(\eta)}\, d\eta \right.$$

$$+ \sum_{m=1}^{\infty} \frac{2}{\left[1 + \left(\frac{4m\pi}{Pe}\right)^2\right]^{1/2}} \left(\int_{\eta_1}^{\Phi} \frac{\exp\left[\frac{Pe}{4}(\Phi - \eta)\left\{1 - \left[1 + \left(\frac{4m\pi}{Pe}\right)^2\right]^{1/2}\right\}\right]}{U_L(\eta)} d\eta \right.$$

$$\left. \left. + \int_{\Phi}^{\eta_2} \frac{\exp\left[-\frac{Pe}{4}(\eta - \Phi)\left\{1 + \left[1 + \left(\frac{4m\pi}{Pe}\right)^2\right]^{1/2}\right\}\right]}{U_L(\eta)} d\eta \right) \right] \tag{29}$$

where for the case in figure 3

$$\eta_1 = 0 \qquad \text{and} \quad \eta_2 = \infty$$

and for the case in figure 5

$$\eta_1 = -\frac{1}{\pi} \ln\left(\frac{1 + k}{1 - k}\right) \qquad \text{and} \qquad \eta_2 = \frac{1}{\pi} \ln\left(\frac{1 + k}{1 - k}\right)$$

Except at the value $\eta_2 = \infty$, the $U_L(\eta)$ is zero at the η_1 and η_2 as these correspond to the jet stagnation points or central point on the plate of the recirculation region. Although the integrands become infinite, the singularities are integrable. For example, for small η the $U_L(\eta)$ in equation (26) becomes

$$U_L(\eta) = \left(\eta - \frac{\eta^3}{3} + \ldots\right)^{(1+\beta)/2} = \eta^{(1+\beta)/2} \qquad \eta \ll 1$$

Then with $\eta_1 = 0$ the first integral in equation (29) can be written by using a small ϵ

$$\int_{\eta=0}^{\Phi} \frac{d\eta}{U_L(\eta)} = \int_{\eta=0}^{\epsilon} \frac{d\eta}{\eta^{(1+\beta)/2}} + \int_{\epsilon}^{\Phi} \frac{d\eta}{U_L(\eta)} = \frac{2}{1-\beta}\epsilon^{(1-\beta)/2} + \int_{\epsilon}^{\Phi} \frac{d\eta}{U_L(\eta)}$$

This form shows that there is no starting difficulty in the integration and that the correct solution can be obtained by starting a small ϵ away from the limit where U_L goes to zero. This type of behavior is true at all the limits where $U_L \to 0$. For example for the infinite row of jets the first integral becomes

$$\int_{\eta_1}^{\Phi} \frac{d\eta}{U_L(\eta)} = \frac{4\epsilon^{1/2}}{\sqrt{\pi k}} + \int_{\eta_1+\epsilon}^{\Phi} \frac{d\eta}{U_L(\eta)}$$

where

$$\eta_1 = -\frac{1}{\pi} \ln\left(\frac{1+k}{1-k}\right)$$

Wall temperatures for large values of L. - For the geometry in figure 3 a solution of simple form can be obtained for large values of L. This is done in appendix D. In figure 20, which is used in that analysis, it is noted that for large L (where $L = \ell/b$) the inviscid jet flow becomes a uniform flow with thickness b. The free streamline boundary is assumed insulated, and the wall has a uniform heat input. Thus for large L the system can be analyzed as a channel flow with uniform heat input. A heat balance starting from $L = 0$ determines the mean temperature at any L. The resulting wall temperature for large L is

$$T_w(L) - T_\infty = \frac{2}{Pe} L + \frac{1}{3} \tag{30}$$

It is noted that this is independent of the angle β of the plate.

Local Nusselt number. - The local heat-transfer behavior can also be expressed as a local heat-transfer coefficient or Nusselt number. The local heat-transfer coefficient is

$$h = \frac{q_w}{t_w - t_\infty} \tag{31}$$

Then the local Nusselt number based on the jet width 2b is

$$Nu(L) = \frac{h2b}{\kappa} = \frac{q_w 2b}{\kappa(t_w - t_\infty)} = \frac{2}{T_w(L) - T_\infty} \tag{32}$$

RESULTS AND DISCUSSION

Jet Flow Into or Over a Corner

The free streamlines of the jet were calculated from equations (2) and (3) for various angles of the impingement plate. (The plate angle γ or corner angle δ are defined in fig. 1.) Results are given in figure 7 for positive and negative plate angles. The case $\gamma = 0$ corresponds to impingement from the normal direction against a flat plate. For $\gamma = -\pi/2$ the heated wall is parallel to the jet and is along the jet centerline. In this instance there is no impingement as the flow direction is parallel to the wall. Figure 7(a) shows that the penetration of the flow into the corner region between the plates becomes poor as the included angle δ between the plates is decreased. This will yield decreased heat-transfer performance for small values of δ (large positive values of γ).

Figure 8 shows the wall temperature variation computed from equation (29) for impingement against plates at various angles. Since the plate is uniformly heated, a region of poor heat transfer in the vicinity of the stagnation point yields a high wall temperature in that region. As the angle γ is increased, there is a rapid increase in temperature at the stagnation point $\ell = 0$. This behavior would be expected from the free streamlines in figure 7(a). For $\gamma = 60^\circ$ the large distance between the free streamline and the origin indicates a very low flow velocity in the corner region. The parts (a) to (d) of figure 8 correspond to the jet Péclet numbers, 5, 10, 20, and 50. An increase in Péclet number can be regarded as an increase in jet velocity. An increased velocity produces

improved heat transfer; hence, the plate temperature decreases as the Péclet number increases. As shown by the final result in appendix D the dimensionless temperature for large L depends only on L and the Péclet number. Hence, all the curves for each part of figure 8 go toward the same limiting line as the L is increased and this line approaches the line predicted in appendix C.

The results shown in figure 9 are a continuation of those in figure 8. In this instance the plate angles γ are negative ($\delta > 180^{\circ}$) so that the flow is over the outside of the heated corner. The heat transfer improves continuously as the plate angle becomes more negative, with the best heat transfer being when the flow is parallel to the heated plates, that is, when $\gamma = -90^{\circ}$.

The heat-transfer characteristics at the stagnation point are examined more completely in figures 10 and 11. Figure 10 gives the dimensionless wall temperatures at the stagnation point as a function of plate angle, each curve being for a different Péclet number. For a fixed Pe the wall temperature increases continuously with γ as a result of the decreasing local velocities in the vicinity of the stagnation region.

As given by equation (32), the Nusselt number is proportional to the reciprocal of the dimensionless wall temperature. Figure 11 gives the ratio of the heat-transfer coefficient at the stagnation point for flow into or over a corner as compared with that for impingement against a flat plate. This shows quite well the significant decrease in heat-transfer coefficient as the geometry varies from flow parallel to a flat plate ($\gamma = -90^{\circ}$) to a jet impinging into a vee groove with total internal angle δ of 60° ($\gamma = 60^{\circ}$). For the case of flow parallel to the plate ($\gamma = -90^{\circ}$), the usual boundary-layer solution for the energy equation gives an infinite heat-transfer coefficient at the leading edge. This is a consequence of neglecting axial heat conduction, which means that the fluid contacting the leading edge is at the free-stream temperature and the thermal boundary layer at the leading edge is of zero thickness. The present analysis however, includes axial conduction in the liquid metal so that some heat is conducted upstream into the fluid before its arrival at the leading edge. This yields a finite heat-transfer coefficient at the leading edge, L = 0.

Infinite Row of Impinging Jets

Figure 12 shows the jet free streamlines for several spacings between adjacent slot jets in an infinite row. As shown by figure 2 the region in figure 12 is between the two centerlines for an incident jet and an adjacent recirculation region. These centerlines are at $X = \pm S/2b$ and are shown as an example in figure 12 for $S/b = 5.2$; to simplify the figure the centerlines have been omitted for the other S/b values. As shown by the analysis in appendix C, the free streamline at $X = 0$ moves upward to an infinite Y value as S/b approaches 4 so that within the constraint of potential flow for $S/b \rightarrow 4$

the region between the jet and adjacent recirculation region becomes completely filled with fluid. At large spacings the recirculation region will not affect the incoming jet flow. (This condition has been reached to a good approximation when $S/b = 8.$)

The wall temperature distributions for impingement on a uniformly heated plate are shown in figure 13 for various spacings and jet Péclet numbers. The best heat transfer is at the stagnation point of the incident jet ($\ell = 0$ in fig. 2 or $L = 0$ in fig. 5), and poor heat transfer is obtained at the center of the recirculation region. The wall temperature at the center of the recirculation region goes through a minimum as the spacing is increased. This results from the improved flow distribution as indicated by figure 12; for larger spacings this is counteracted by the greater extent of the heated region, and the temperature rises with spacing. The results for a single jet, which correspond to an infinite spacing, are from reference 2. For a spacing S/b of 6.4 the results in the vicinity of the incident stagnation region are within a few percent of the values for infinite spacing.

Figure 14 shows the Nusselt number at the stagnation point of the incident jet ($L = 0$ in fig. 5). As shown by the free streamlines in figure 12 the jets significantly interfere with each other for S/b less than about 5.2, causing a thickening of the flow region and hence lower velocities in the vicinity of the heated plate. Figure 14 shows how the heat transfer becomes poorer as this interference increases with decreased jet spacing. As S/b approaches four, the Nusselt number decreases toward zero as the region between the jet and adjacent recirculation region becomes filled with fluid.

CONCLUSIONS

The flow in an impinging two-dimensional free jet (a single jet or one jet of an infinite row) is bounded by free streamlines and solid boundaries or symmetry lines which are also streamlines. As a result of being bounded by streamlines, the jet region maps into a parallel flow region in a system using streamline coordinates. When the energy equation is transformed into the streamline coordinate system, it becomes the same as the equation for convection to a uniform flow in a parallel plate channel. This equation can be solved by known analytical techniques, and the solution is then mapped back into the physical plane. Thus the analysis combines the conformal mapping technique for free jets with a transformation of the energy equation to reduce the problem to one having a standard type of solution.

Heat transfer results are obtained for two geometries. The first is for a jet impinging either into a corner region formed at the apex of two uniformly heated plates at an angle to each other or flowing over the exterior of the corner region. The second is for an infinite row of parallel jets impinging against a uniformly heated plate.

The heat transfer for flow into a corner becomes quite poor as the included angle between the heated plates is decreased because a large region of low velocity is formed. Results are given to illustrate the continuous decrease in heat-transfer performance as the geometry is changed from flow over the outside of a corner (included angle $> 180^{\circ}$) to flow against a flat plate (included angle = 180°) and then into an internal corner (included angle $< 180^{\circ}$).

In a similar fashion the heat-transfer performance decreases for a row of impinging jets as the spacing between jets decreases. When the ratio of spacing between jets to jet width increases beyond about 6, the heat-transfer behavior near the impingement stagnation point becomes close to that for a single jet.

Lewis Research Center,
National Aeronautics and Space Administration,
Cleveland, Ohio, August 1, 1975,
505-04.

APPENDIX A

SYMBOLS

b	half width of incident jet far from plate
C_p	specific heat of fluid
$\mathscr{C}_1$	constant evaluated in eq. (D6)
$\mathscr{C}_2, \mathscr{C}_3$	constants of integration
cn, dn, sn	elliptic functions
f	function of coordinate n_w
h	local heat-transfer coefficient along plate
$\hat{i}, \hat{j}$	unit vector in x and y directions
K	complete elliptic integral of first kind
K'	complete elliptic integral $K' = K(k')$
k	modulus of elliptic function
k'	complementary modulus, $k' = \sqrt{1 - k^2}$
L	dimensionless coordinate, ℓ/b
ℓ	coordinate along heated plate measured from impingement stagnation point
m	integer
N	dimensionless normal coordinate, n/b
Nu	Nusselt number, $h2b/\kappa$
n	normal coordinate
$\hat{n}$	unit normal vector
Pe	jet Péclet number, $\lvert v_\infty \rvert 2b/\alpha$
Pr	fluid Prandtl number, $C_p \mu/\kappa$
q_w	heat flux specified at wall
Re	jet Reynolds number, $\lvert v_\infty \rvert 2b\rho/\mu$
S	half spacing between jets
T	dimensionless temperature, t_κ/bq_w; variable in auxiliary T-plane
t	temperature; variable in auxiliary t-plane, $t = \xi - i\eta$
$\bar{t}$	mixed mean fluid temperature

U, V dimensionless velocities, $u/|v_\infty|$, $v/|v_\infty|$

u velocity in x direction; variable in auxiliary u-plane

v velocity in y direction

$\vec{u}$ local fluid velocity vector

W complex potential $W = \Phi + i\Psi$

X, Y dimensionless coordinates, x/b and y/b

x, y rectangular coordinates

Z complex variable, $Z = X + iY$

α thermal diffusivity of fluid, $\kappa/\rho C_p$

β plate angle $\beta = \gamma/(\pi/2)$

γ plate angle measured from direction normal to jet, see fig. 1

δ total included corner angle (defined in fig. 1)

ϵ a small number

ζ complex velocity, $\zeta = U - iV$

η dummy variable of integration; ordinate in auxiliary t-plane

θ angle in auxiliary t-plane (defined in fig. 16)

κ thermal conductivity of fluid

μ fluid viscosity

ν fluid kinematic viscosity (viscous diffusivity), μ/ρ

ξ abscissa in auxiliary t-plane

ρ fluid density

Φ dimensionless potential, $\varphi/|v_\infty|b$

φ potential function

Ψ dimensionless stream function, $\psi/|v_\infty|b$

ψ stream function

∇ gradient, $\nabla = \hat{i}\frac{\partial}{\partial x} + \hat{j}\frac{\partial}{\partial y}$

$\tilde{\nabla}$ dimensionless gradient, $\tilde{\nabla} = \hat{i}\frac{\partial}{\partial X} + \hat{j}\frac{\partial}{\partial Y}$

Subscripts:

L along heated wall

o reference value at $\theta = \pi/4$

s at free streamline

w at wall

∞ condition of undisturbed incoming fluid

APPENDIX B

MAPPING FOR JET FLOW IN A CORNER

Mapping of Flow Between Physical and Potential Planes

The flow being considered here is steady, incompressible, inviscid and irrotational. The region surrounding the jet is at constant pressure so that the outer jet boundary is a free streamline. The details of this type of flow, such as the velocity along the impingement plate and the shape of the free streamlines, can be obtained by conformal mapping (ref. 4). A dimensionless system of variables is used as defined in appendix A. Additional information on this type of solution is in reference 2.

The flow is expressed in terms of a complex potential:

$$W = \Phi + i\Psi \tag{B1}$$

The derivative of Φ in a direction gives the local velocity in that direction, and the derivatives of Ψ are related to the derivatives of Φ by the Cauchy-Riemann relations.

The derivative of the complex potential W provides the complex conjugate of the velocity in the flow region,

$$\frac{dW}{dZ} = U - iV = \zeta \tag{B2}$$

By integrating, the relation between the physical plane and the potential plane is found as

$$Z = \int \frac{1}{\zeta} dW + \text{constant} \tag{B3}$$

The known conditions of the flow can be used to determine the flow regions in the ζ and W coordinate planes. To integrate equation (B3) these ζ and W regions are each mapped conformally into an intermediate t plane. Once the $W(t)$ and $\zeta(t)$ conformal transformations are known, they can be substituted into equation (B3) and $Z(t)$ obtained by integration. The integration constant is evaluated by matching a point in the t and Z planes. The conditions in the flow, such as the velocity, are then known as a function of position implicitly through the variable t.

Hodograph Plane and Transformation to Auxiliary t-Plane

The flow region in the hodograph plane is shown in figure 15. The free streamline is in a region of constant pressure and hence has a constant velocity magnitude along it which is equal to unity by virtue of the dimensionless velocity at point 2. Hence, the free streamline transforms into part of a unit circle in the ζ-plane. The velocity is zero at point 4, and the velocity direction must be along the axis of symmetry $\widehat{34}$ and along the plate $\widehat{45}$. The hodograph is thus a sector of a unit circle.

A convenient geometry for the intermediate t plane is a quarter circle as shown in figure 16. The mapping between the ζ- and t-planes is given by (ref. 4)

$$\zeta(t) = t^{1+\beta} e^{-i\beta\pi/2} \tag{B4}$$

Potential Plane and Transformation to Auxiliary t-Plane

From one of the Cauchy-Riemann equations and the definition of velocity potential

$$\frac{\partial \Psi}{\partial X} = -\frac{\partial \Phi}{\partial Y} = -V \tag{B5}$$

Between points 3 and 2 in figure 3(b) $V = -1$ so that by integrating

$$\Psi(2) - \Psi(3) = \int_{X(3)}^{X(2)} -V \, dX = \int_{X(3)}^{X(2)} dX = 1 \tag{B6}$$

The $\Psi(3)$ is arbitrarily set equal to zero and then $\Psi(2) = 1$. The line $\widehat{345}$ is thus the zero streamline, and the free streamline $\widehat{12}$ is the unit streamline. The potential plane as shown in figure 4 is thus an infinitely long strip of unit width.

The transformation of a unit strip (W-plane) into a quarter circle (t-plane) is given by

$$W(t) = \frac{2}{\pi} \ln\left(\frac{1 + t^2}{1 - t^2}\right) \tag{B7}$$

Integral to Determine Z(t)

Noting that the condition $Z = 0$ when $t = 0$ (point 4 in figs. 3(b) and 16) yields a zero integration constant, the relation in equation (B3) can be written as

$$Z = \int_0^t \frac{1}{\zeta(t)} \frac{dW}{dt}\, dt \tag{B8}$$

Differentiating the $W(t)$ in equation (B7) gives

$$\frac{dW}{dt} = \frac{8t}{\pi(1 - t^4)}$$

Then

$$Z = \int_0^t \frac{e^{i\beta(\pi/2)}}{t^{1+\beta}} \frac{8t}{\pi(1 - t^4)}\, dt = \frac{8}{\pi} e^{i\beta(\pi/2)} \int_0^t \frac{dt}{t^{\beta}(1 - t^4)} \tag{B9}$$

Along the heated plate $\widehat{45}$ the t is real and equal to ξ so that

$$Z = \frac{8}{\pi} e^{i\beta(\pi/2)} \int_0^{\xi} \frac{d\xi}{\xi^{\beta}(1 - \xi^4)} \qquad Z \text{ on } \widehat{45} \tag{B10}$$

The coordinate L along the plate is related to Z by

$$Z = Le^{i\beta(\pi/2)} \tag{B11}$$

Hence the L along the plate is given by

$$L = \frac{8}{\pi} \int_0^{\xi} \frac{d\xi}{\xi^{\beta}(1 - \xi^4)} \qquad L \text{ along } \widehat{45} \tag{B12}$$

To relate L to Φ, equation (B7) gives along $\widehat{45}$ where $t = \xi$

$$W = \Phi + i\Psi = \frac{2}{\pi} \ln\left(\frac{1 + \xi^2}{1 - \xi^2}\right)$$

and since ξ is real this gives

$$\Phi = \frac{2}{\pi} \ln\left(\frac{1 + \xi^2}{1 - \xi^2}\right) \tag{B13}$$

This can be rearranged into the form

$$\Phi = \frac{4}{\pi} \tanh^{-1}(\xi^2) \qquad 0 \leq \xi \leq 1 \tag{B14}$$

Equations (B12) and (B14) relate L to Φ by use of the intermediate variable ξ; this relation will be needed to transform the wall temperatures obtained in the W-plane into the physical plane.

Free Streamline

To obtain the equations for the free streamline $\widehat{12}$, it is noted that the streamline is along the unit circle in figure 16 so that

$$t = (1)e^{i\theta} \qquad 0 \leq \theta \leq \frac{\pi}{2}$$

Since the streamline starts and ends at infinity it is convenient to start the integration for Z in equation (B9) at a point X_o, Y_o (corresponding to θ_o) on the streamline. (The X_o, Y_o will be determined later.) Using equation (B9) and the fact that along the streamline $dt = ie^{i\theta}\, d\theta$ gives

$$Z - Z_o = \frac{8}{\pi} e^{i\beta(\pi/2)} \int_{\theta_o}^{\theta} \frac{ie^{i\theta}}{e^{i\beta\theta}(1 - e^{i4\theta})}\, d\theta$$

where Z_o is the value of Z at $\theta = \theta_o$. To simplify this expression multiply the numerator and denominator by $e^{-i2\theta}$ to obtain

$$Z - Z_o = \frac{8}{\pi} e^{i\beta(\pi/2)} \int_{\theta_o}^{\theta} \frac{ie^{-i\theta}}{e^{i\beta\theta}(e^{-i2\theta} - e^{i2\theta})} d\theta$$

$$Z - Z_o = \frac{8}{\pi} e^{i\beta(\pi/2)} \int_{\theta_o}^{\theta} \frac{ie^{-i\theta}}{e^{i\beta\theta}(-2i \sin 2\theta)} d\theta$$

$$Z - Z_o = -\frac{4}{\pi} \int_{\theta_o}^{\theta} \frac{e^{-i\left[\theta(1+\beta) - \beta\frac{\pi}{2}\right]}}{\sin 2\theta} d\theta$$

Separating real and imaginary parts

$$X - X_o = -\frac{4}{\pi} \int_{\theta=\theta_o=\pi/4}^{\theta} \frac{\cos\left[\theta(1+\beta) - \beta\frac{\pi}{2}\right]}{\sin 2\theta} d\theta \qquad 0 \le \theta \le \frac{\pi}{2} \qquad \text{(B15a)}$$

$$Y - Y_o = \frac{4}{\pi} \int_{\theta=\theta_o=\pi/4}^{\theta} \frac{\sin\left[\theta(1+\beta) - \beta\frac{\pi}{2}\right]}{\sin 2\theta} d\theta \qquad 0 \le \theta \le \frac{\pi}{2} \qquad \text{(B15b)}$$

where the point X_o, Y_o has been chosen at $\theta_o = \pi/4$ as a convenient point along the streamline.

To determine X_o, Y_o, equation (B8) will be integrated from $Z = 0$, $t = 0$ to $Z = Z_o$, $t = e^{i\theta}$. It is convenient to carry out the integration along a line of constant $\theta = \theta_o$. Then

$$t = |t| e^{i\theta_o}$$

$$dt = d|t|e^{i\theta_o}$$

and

$$Z_o = \frac{8}{\pi} e^{i\beta(\pi/2)} \int_{|t|=0}^{1} \frac{e^{i\theta_o}\, d|t|}{|t|^{\beta} e^{i\beta\theta_o}(1 - |t|^4 e^{i4\theta_o})}$$

Letting $\theta_o = \pi/4$

$$Z_o = \frac{8}{\pi} e^{i\beta(\pi/4)} e^{i(\pi/4)} \int_{|t|=0}^{1} \frac{d|t|}{|t|^{\beta}(1 + |t|^4)}$$

Separating into real and imaginary parts

$$X_o = \frac{8}{\pi} \cos\left[\frac{\pi}{4}(1 + \beta)\right] F(\beta) \qquad \text{(B 16a)}$$

$$Y_o = \frac{8}{\pi} \sin\left[\frac{\pi}{4}(1 + \beta)\right] F(\beta) \qquad \text{(B 16b)}$$

where

$$F(\beta) = \int_0^1 \frac{d\eta}{\eta^{\beta}(1 + \eta^4)}$$

Velocity Along Plate

Along the plate $\widehat{45}$ the velocity must be tangential to the surface so that

$$\zeta = U - iV = |\vec{U}| e^{-i\beta(\pi/2)}$$

Also along $\widehat{45}$, $t = \xi$ so from equation (B4)

$$\zeta = \xi^{1+\beta} e^{-i\beta(\pi/2)}$$

Hence, along the plate

$$|\vec{U}| = U_L = \xi^{1+\beta}$$

Then using equation (B14)

$$U_L = \left[\tanh\left(\frac{\pi\Phi}{4}\right)\right]^{(1+\beta)/2} \qquad \text{(B17)}$$

APPENDIX C

MAPPING FOR INFINITE ROW OF JETS

From the periodic nature of the flow in figure 2, it is necessary to consider only the portion of the flow between the two centerlines on either side of the y-axis. This portion is shown in the dimensionless physical plane in figure 5.

The corresponding hodograph is shown in figure 17. The magnitude of the flow velocity is unity along the free streamline $\widehat{345}$; hence this line transforms into a unit semicircle in the hodograph plane. Along the centerlines $\widehat{12}$ and $\widehat{67}$ the U velocity component is zero, and along the heated plate $\widehat{781}$ the V component is zero. The velocity is zero at the impingement and reverse stagnation points 7 and 1.

In the potential plane (fig. 6) the free streamline becomes a horizontal line. Parallel to it is the streamline $\widehat{6712}$ formed by the centerlines and the heated plate. Thus the flow region transforms into a strip of unit width. The physical coordinates are related to the hodograph and potential coordinates as previously derived in equation (B3).

$$Z = \int \frac{1}{\zeta} dW + \text{constant} \tag{B3}$$

To relate ζ and W in order to carry out the integration, the auxiliary u plane in figure 18 is used in which the flow region is mapped into a rectangle. The relation between ζ and u can be obtained from results in reference 4 as

$$\zeta(u) = \frac{k \operatorname{cn} u}{k' + \operatorname{dn} u} \tag{C1}$$

where

$$k'^2 = 1 - k^2$$

The mapping between the W and u planes is derived by use of the intermediate T plane in figure 19. The W is related to T by

$$W = \frac{1}{\pi} \ln \left(\frac{\frac{1}{k} + T}{\frac{1}{k} - T} \right) \tag{C2}$$

The transformation between T and u is by means of an elliptic function:

$$T = \text{sn } u \tag{C3}$$

Equation (B3) is written in terms of u as

$$Z = \int \frac{1}{\zeta(u)} \frac{dW}{du} du + \text{const}$$

Substitute sn u for T in equation (C2) and differentiate to obtain

$$\frac{dW}{du} = \frac{2}{\pi k} \frac{\text{cn } u \text{ dn } u}{\frac{1}{k^2} - \text{sn}^2 u}$$

Then

$$Z = \frac{2}{\pi} \int \frac{k' + \text{dn } u}{k \text{ cn } u} \frac{k \text{ cn } u \text{ dn } u}{1 - k^2 \text{sn}^2 u} du + \text{const}$$

Using the identity $1 - k^2 \text{sn}^2 u = \text{dn}^2 u$, reduces this to

$$Z = \frac{2}{\pi} \left(\int \frac{k'}{\text{dn } u} du + \int du \right) + \text{const}$$

Integrating yields

$$Z = \frac{2}{\pi} \left[\tan^{-1} \left(\frac{k' \text{ sn } u}{\text{cn } u} \right) + u \right] \tag{C4}$$

where the integration constant has been set equal to zero by use of the condition at point 8 that Z = 0 when u = 0. The spacing between the jets is related to K (and hence to k) by the fact that at u = K, Z = S/2b. Then from equation (C4),

$$\frac{S}{2b} = \frac{2}{\pi} \left(\frac{\pi}{2} + K \right) \quad \text{or} \quad K = \frac{\pi}{2} \left(\frac{S}{2b} - 1 \right) \tag{C5}$$

With K determined from a specified S/2b, the k is also known from the definition of the complete elliptic integral,

$$K = \int_0^{\pi/2} \frac{d\varphi}{\sqrt{1 - k^2 \sin^2 \varphi}} \qquad 0 \le k^2 \le 1$$

and the k' is found from

$$k' = \sqrt{1 - k^2}$$

Since the minimum value of the elliptic function K is $\pi/2$, equation (C5) shows that the minimum spacing consistent with potential flow is S/2b = 2. As the spacing is decreased toward this value, it will be shown that the free streamline moves out toward infinite distance above the heated plate; that is, the space between the jets completely fills with fluid.

Coordinates of Free Streamline

From figure 18 the free streamline corresponds to $u = \xi + iK'$. Substituting into equation (C4) for Z gives

$$Z(\xi + iK') = \frac{2}{\pi}\left[\tan^{-1}\left(\frac{k'i}{dn\ \xi}\right) + \xi + iK'\right]$$

which is equivalent to

$$X + iY\Big|_S = \frac{2}{\pi}\left[\frac{i}{2}\ln\left(\frac{dn\ \xi + k'}{dn\ \xi - k'}\right) + \xi + iK'\right]$$

The X, Y coordinates along the free streamline are then

$$X = \frac{2}{\pi}\xi \qquad -K \le \xi \le K \tag{C6a}$$

$$Y = \frac{2}{\pi}\left[K' + \frac{1}{2}\ln\left(\frac{dn\ \xi + k'}{dn\ \xi - k'}\right)\right] \qquad -K \le \xi \le K \tag{C6b}$$

Tangential Velocity and Relation Between Φ and X Along Heated Wall

The solution of the energy equation involves the tangential velocity along the heated wall. Also the Φ along the heated plate in the potential plane has to be related to the X location in the physical plane.

Along the heated plate $\widehat{71}$, $-S/2b \leq X \leq S/2b$, $Y = 0$, the $u = \xi$ with the range $-K \leq \xi \leq K$. Then along the plate, equation (C4) becomes

$$X = \frac{2}{\pi}\left[\tan^{-1}\left(\frac{k' \operatorname{sn} \xi}{\operatorname{cn} \xi}\right) + \xi\right] \tag{C7}$$

Along the heated plate $\Psi = 0$ so that $W = \Phi$. Also $u = \xi$ so that from equation (C3) $T = \operatorname{sn} \xi$. Then using equation (C2)

$$\Phi = \frac{1}{\pi} \ln\left(\frac{1 + k \operatorname{sn} \xi}{1 - k \operatorname{sn} \xi}\right) \tag{C8}$$

Equations (C7) and (C8) relate the Φ and X through the use of the intermediate variable ξ. At point 1, $\xi = K$ so that $\operatorname{sn} \xi = 1$ and then

$$\Phi \text{ (point 1)} = \frac{1}{\pi} \ln\left(\frac{1 + k}{1 - k}\right) \tag{C9a}$$

At point 7, $\xi = -K$ so that $\operatorname{sn} \xi = -1$ and then

$$\Phi \text{ (point 7)} = \frac{1}{\pi} \ln\left(\frac{1 - k}{1 + k}\right) = -\Phi \text{ (point 1} \tag{C9b}$$

From equation (C1), since the V component is zero along the plate, the U component along the plate becomes

$$U = \frac{k \operatorname{cn} \xi}{k' + \operatorname{dn} \xi} \tag{C10}$$

Equation (C8) is solved for $\operatorname{sn} \xi$ to yield

$$\operatorname{sn} \xi = \frac{1}{k} \frac{1 - e^{-\pi\Phi}}{1 + e^{-\pi\Phi}} = \frac{1}{k} \tanh\left(\frac{\pi\Phi}{2}\right)$$

Then using the identities $\mathrm{cn}\,\xi = \sqrt{1 - \mathrm{sn}^2\xi}$ and $\mathrm{dn}\,\xi = \sqrt{1 - k^2\,\mathrm{sn}^2\xi}$, the expression for U along the plate becomes

$$U_L = \frac{\left[k^2 - \tanh^2\left(\frac{\pi\Phi}{2}\right)\right]^{1/2}}{k' + \left[1 - \tanh^2\left(\frac{\pi\Phi}{2}\right)\right]^{1/2}} \qquad \text{(C11)}$$

APPENDIX D

SOLUTION FOR WALL TEMPERATURE AT LARGE ℓ FOR CORNER FLOW

Let the ℓ, n_w coordinate system be along and normal to the impingement plate as shown in figure 20. At large ℓ the flow distribution has become uniform with velocity v_∞. The convective heat-transfer equation in the region of large ℓ is

$$v_\infty \rho C_p \frac{\partial t}{\partial \ell} = \kappa \left(\frac{\partial^2 t}{\partial \ell^2} + \frac{\partial^2 t}{\partial n_w^2} \right) \tag{D1}$$

In this region the temperature distribution has become fully developed, that is, the shape of the temperature profile across the n_w direction is no longer changing with increasing ℓ. As a result of the uniform heat addition at the wall, however, the temperatures across the width of the flow are all increasing linearly with ℓ. The temperature distribution for large ℓ must then have the form

$$t(\ell, n_w) = \mathscr{C}_1 \ell + f(n_w) \tag{D2}$$

This form of the solution is substituted into the energy equation (D1) to yield

$$v_\infty \rho C_p \mathscr{C}_1 = \kappa \frac{d^2 f}{dn_w^2} \tag{D3}$$

To obtain f integrate once to give

$$\frac{df}{dn_w} = \frac{v_\infty \rho C_p}{\kappa} \mathscr{C}_1 n_w + \mathscr{C}_2$$

To satisfy the condition that $df/dn_w = 0$ at the insulated boundary $n_w = b$, the $\mathscr{C}_2 = -\frac{v_\infty \rho C_p \mathscr{C}_1}{\kappa} b$. A second integration then yields

$$f = \frac{v_\infty \rho C_p \mathscr{C}_1}{\kappa} \left(\frac{n_w^2}{2} - b n_w \right) + \mathscr{C}_3 \tag{D4}$$

To obtain $\mathscr{C}_1$ and $\mathscr{C}_3$ an overall heat balance is used from the incoming jet at large y in figure 20 where the fluid is all at t_∞, to a location at large ℓ where the mixed mean fluid temperature is $\bar{t}(\ell)$. The heat balance yields

$$q_w \ell = bv_\infty \rho C_p \left[\bar{t}(\ell) - t_\infty\right] \tag{D5}$$

In the fully developed region from equations (D5) and (D2),

$$\frac{\partial t}{\partial \ell} = \frac{\partial \bar{t}}{\partial \ell} = \frac{q_w}{bv_\infty \rho C_p} = \mathscr{C}_1 \tag{D6}$$

so that the f in equation (D4) becomes

$$f = \frac{q_w}{\kappa b}\left(\frac{n_w^2}{2} - bn_w\right) + \mathscr{C}_3$$

The temperature distribution in equation (D2) becomes

$$t(\ell, n_w) = \frac{q_w \ell}{bv_\infty \rho C_p} + \frac{q_w}{\kappa b}\left(\frac{n_w^2}{2} - bn_w\right) + \mathscr{C}_3 \tag{D7}$$

For a uniform velocity distribution the mixed mean fluid temperature $\bar{t}(\ell)$ is given by

$$\bar{t}(\ell) = \frac{1}{b}\int_0^b t(\ell, n_w) dn_w \tag{D8}$$

Then, substituting equation (D7) into (D8) gives

$$\bar{t}(\ell) = \frac{1}{b}\int_0^b \left[\frac{q_w \ell}{bv_\infty \rho C_p} + \frac{q_w}{\kappa b}\left(\frac{n_w^2}{2} - bn_w\right) + \mathscr{C}_3\right] dn_w$$

$$\bar{t}(\ell) = \frac{q_w \ell}{bv_\infty \rho C_p} - \frac{q_w b}{3\kappa} + \mathscr{C}_3 \tag{D9}$$

Equating this to $\bar{t}(\ell)$ from equation (D5) gives

$$\frac{q_w \ell}{b v_\infty \rho C_p} + t_\infty = \frac{q_w \ell}{b v_\infty \rho C_p} - \frac{q_w b}{3\kappa} + \mathscr{C}_3$$

Hence,

$$\mathscr{C}_3 = t_\infty + \frac{q_w b}{3\kappa} \tag{D10}$$

The fluid temperature distribution in equation (D7) then becomes

$$t(\ell, n_w) = \frac{q_w \ell}{b v_\infty \rho C_p} + \frac{q_w}{\kappa b}\left(\frac{n_w^2}{2} - b n_w\right) + t_\infty + \frac{q_w b}{3\kappa} \tag{D11}$$

To obtain the wall temperature, this is evaluated at $n_w = 0$

$$t_w(\ell) = \frac{q_w \ell}{b v_\infty \rho C_p} + \frac{q_w b}{3\kappa} + t_\infty \tag{D12}$$

In dimensionless form the final result is

$$T_w(L) - T_\infty = \frac{2}{Pe} L + \frac{1}{3} \tag{D13}$$

which is valid for large L. Figure 8 indicates that, depending on the plate angle, L can be in the range of about 2 to 10 to obtain reasonable agreement with the complete solution.

REFERENCES

1. Gardon, Robert; and Akfirat, J. Cahit: Heat Transfer Characteristics of Impinging Two-Dimensional Air Jets. J. Heat Transfer, ASME Trans., vol. 88, Series C, no. 1, Feb. 1966, pp. 101-108.
2. Siegel, Robert: Analysis of Heat Transfer for a Normally Impinging Liquid-Metal Slot Jet. NASA TN D-7260, 1973.
3. Siegel, Robert; and Goldstein, Marvin E.: Analytical Method for Steady State Heat Transfer in Two-Dimensional Porous Media. NASA TN D-5878, 1970.
4. Birkhoff, Garrett; and Zarantonello, E. H.: Jets, Wakes, and Cavities. Academic Press, Inc., 1957.

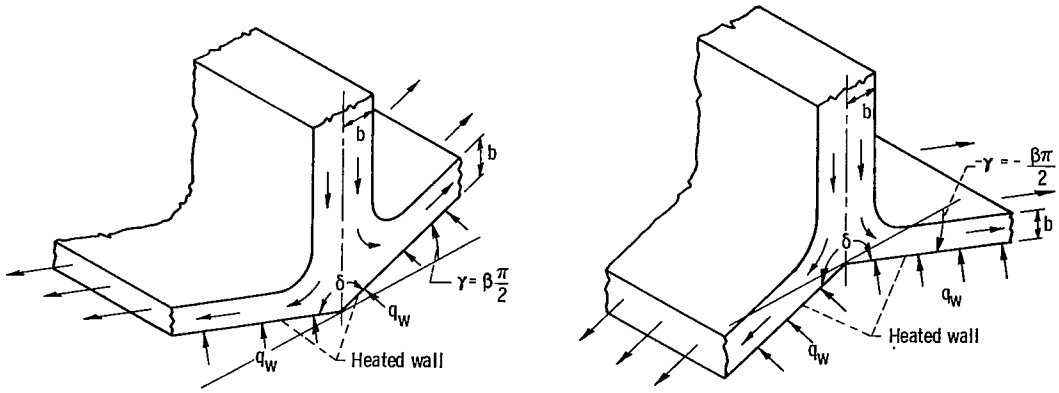

(a) Flow into internal corner (γ positive).

(b) Flow over external corner (γ negative).

Figure 1. - Inviscid-irrotational slot jet impinging in corner region formed at intersection of two uniformly heated plates.

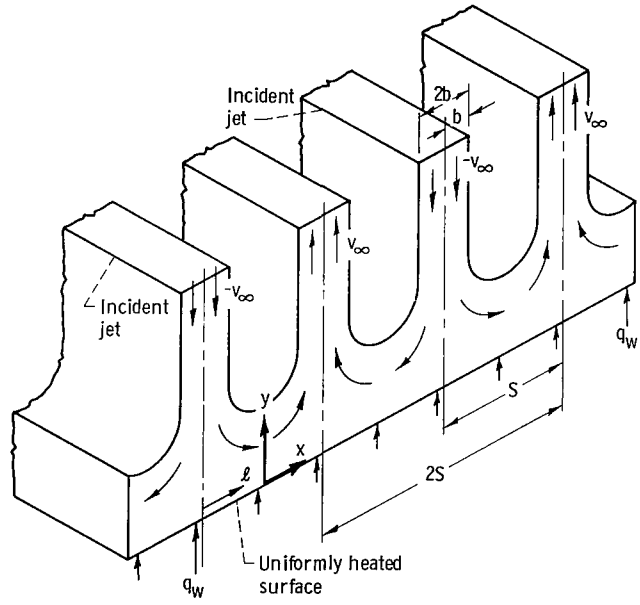

Figure 2. - Impingement of infinite row of liquid-metal slot jets against uniformly heated surface.

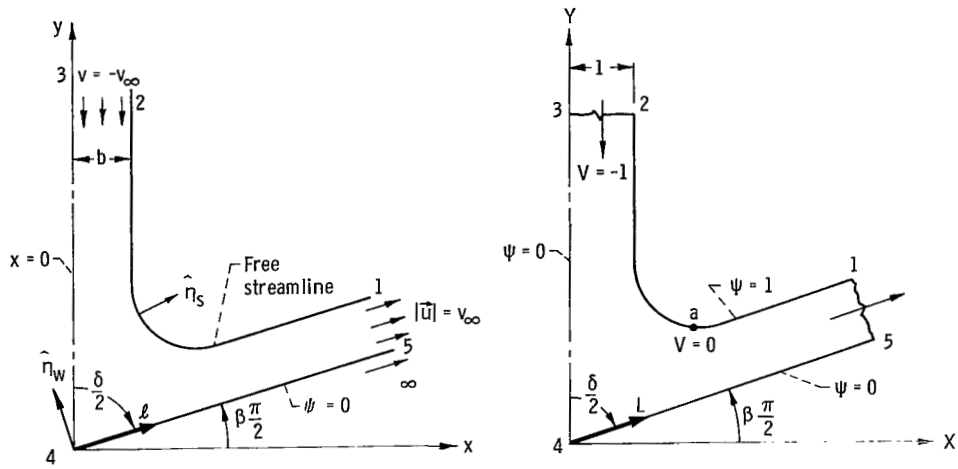

(a) Physical plane. (b) Dimensionless physical plane.

Figure 3. - Jet region in physical plane for impingement in corner.

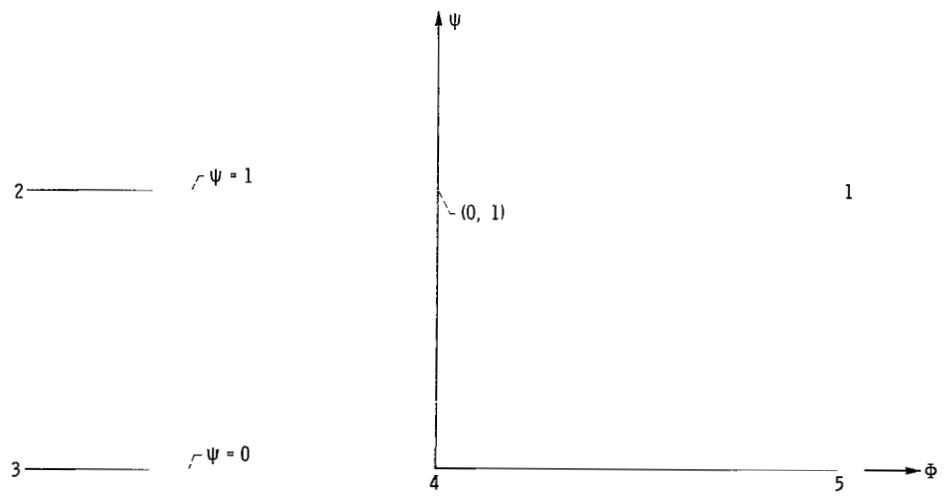

Figure 4. - Jet region and boundary conditions for flow in corner region mapped into potential plane.

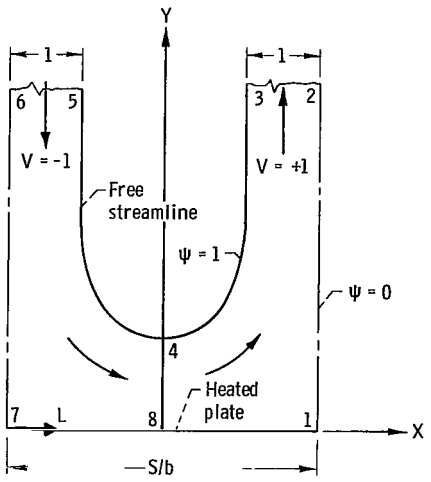

Figure 5. - Jet region in dimensionless physical plane for infinite row of impinging jets.

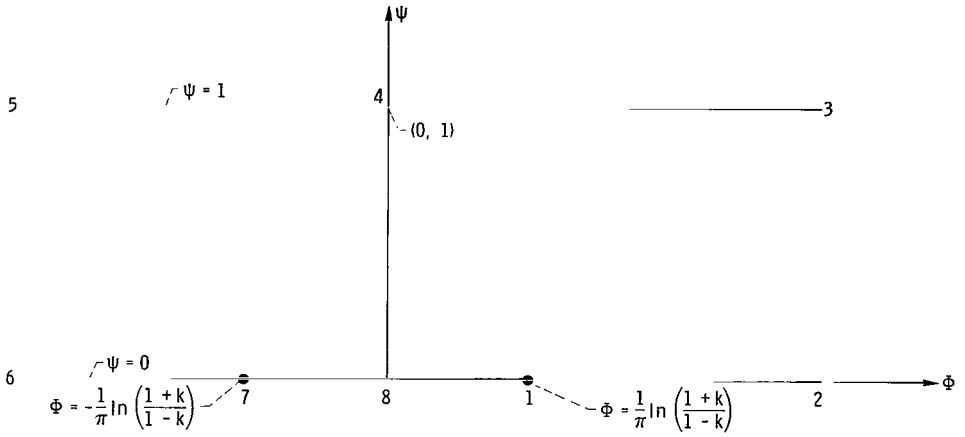

Figure 6. - Jet region and boundary conditions for infinite row of jets mapped into potential plane.

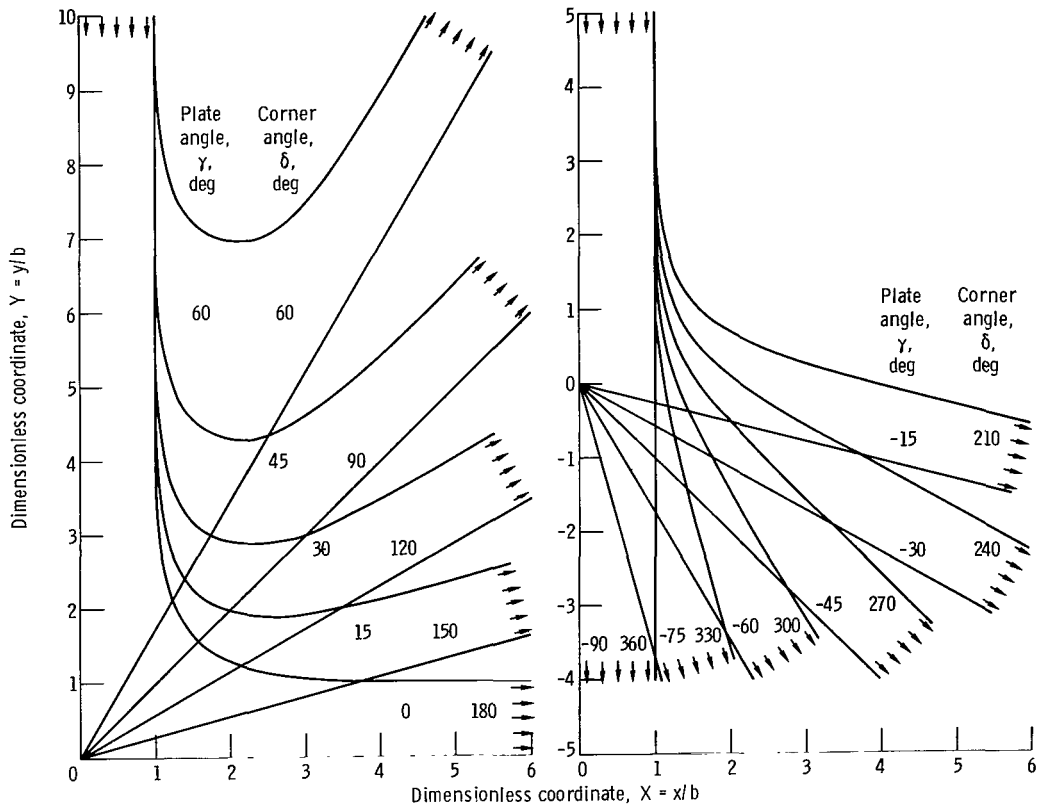

(a) Impingement into internal corner (positive γ). (b) Impingement over an external corner (negative γ).

Figure 7. - Free streamlines for jet impinging in corner region.

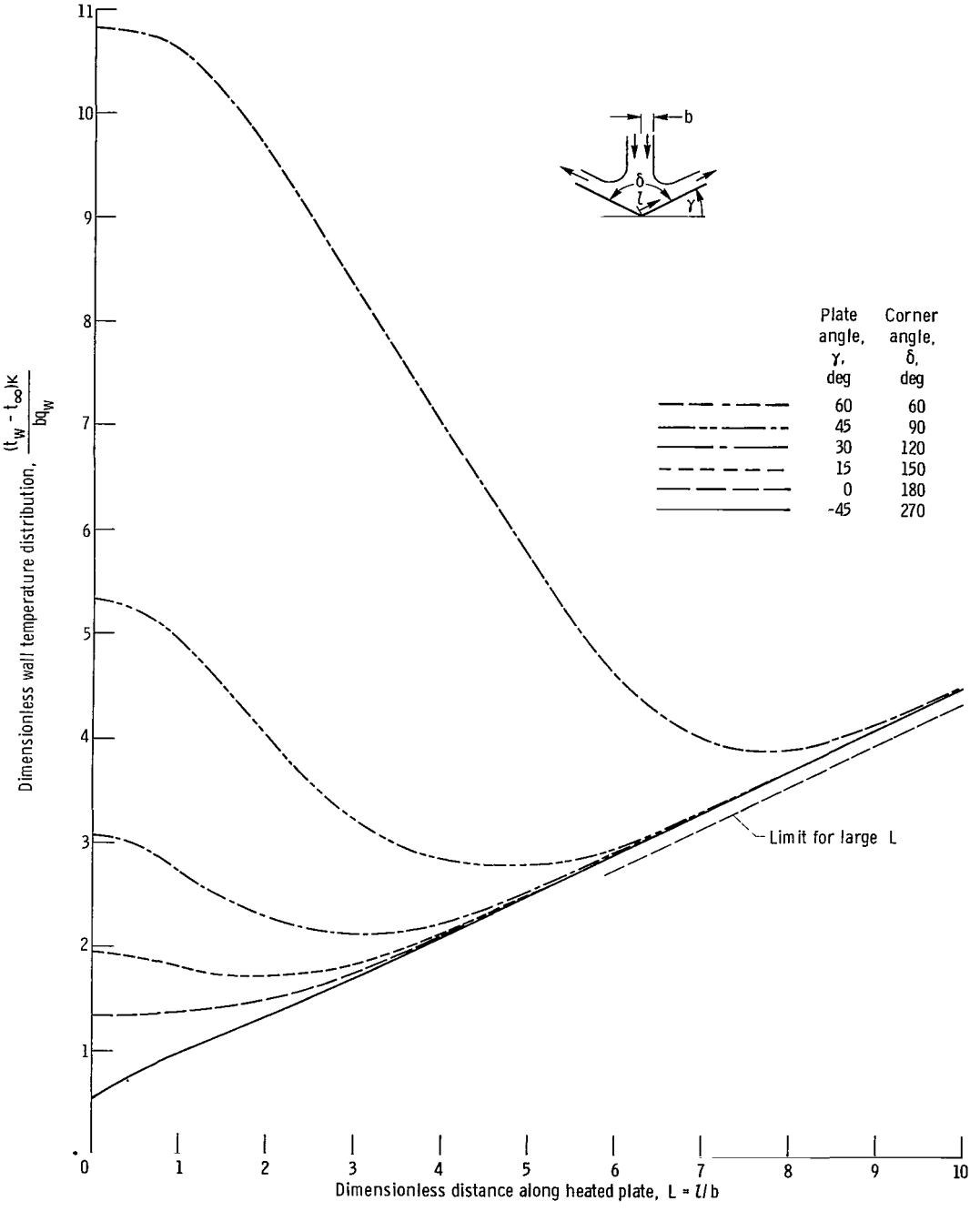

(a) Jet Péclet number, 5.

Figure 8. - Effect of angle of impingement plate on dimensionless wall temperature distribution for fixed value of jet Péclet number at plate angles from -45 to 60°.

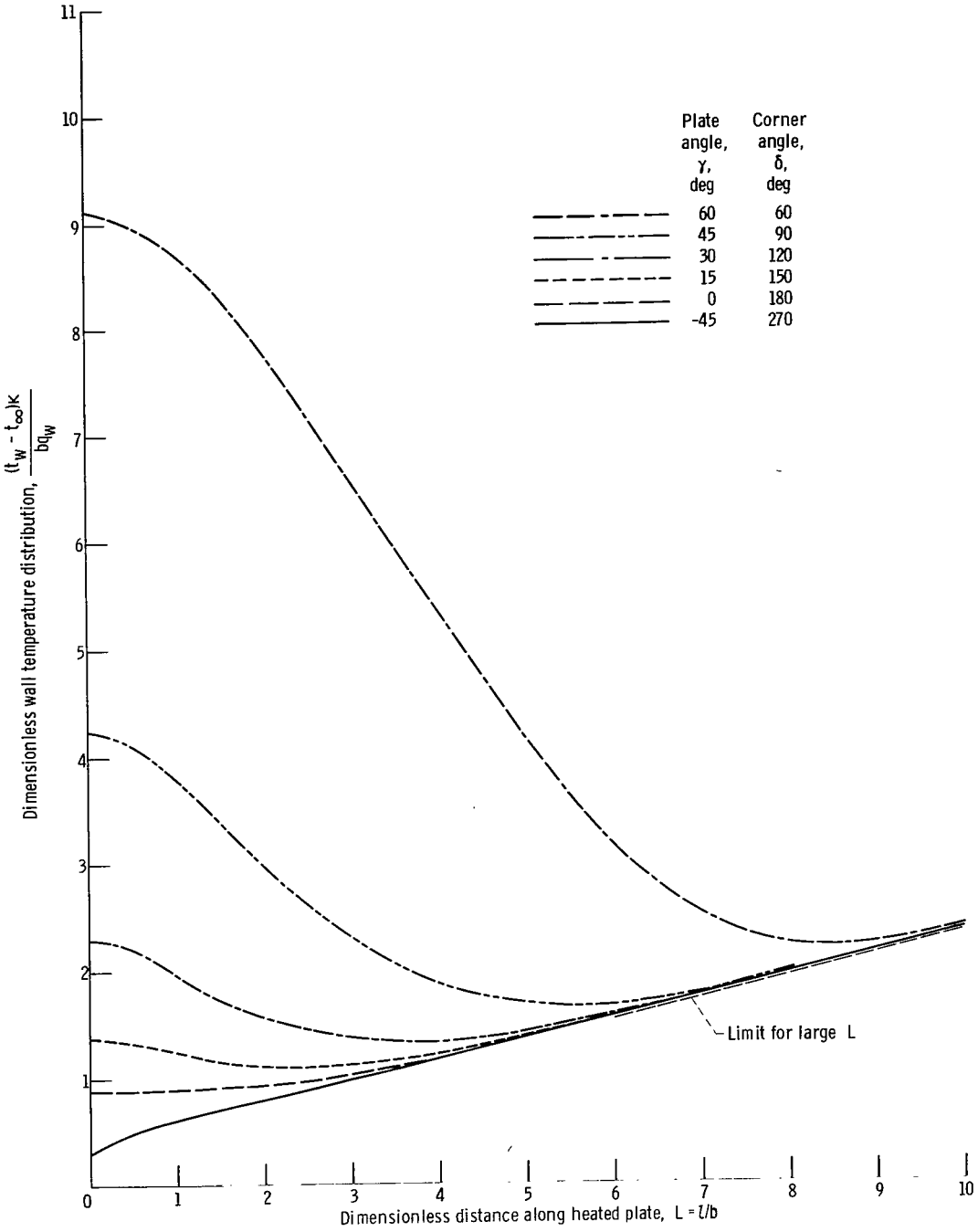

(b) Jet Péclet number, 10.

Figure 8. - Continued.

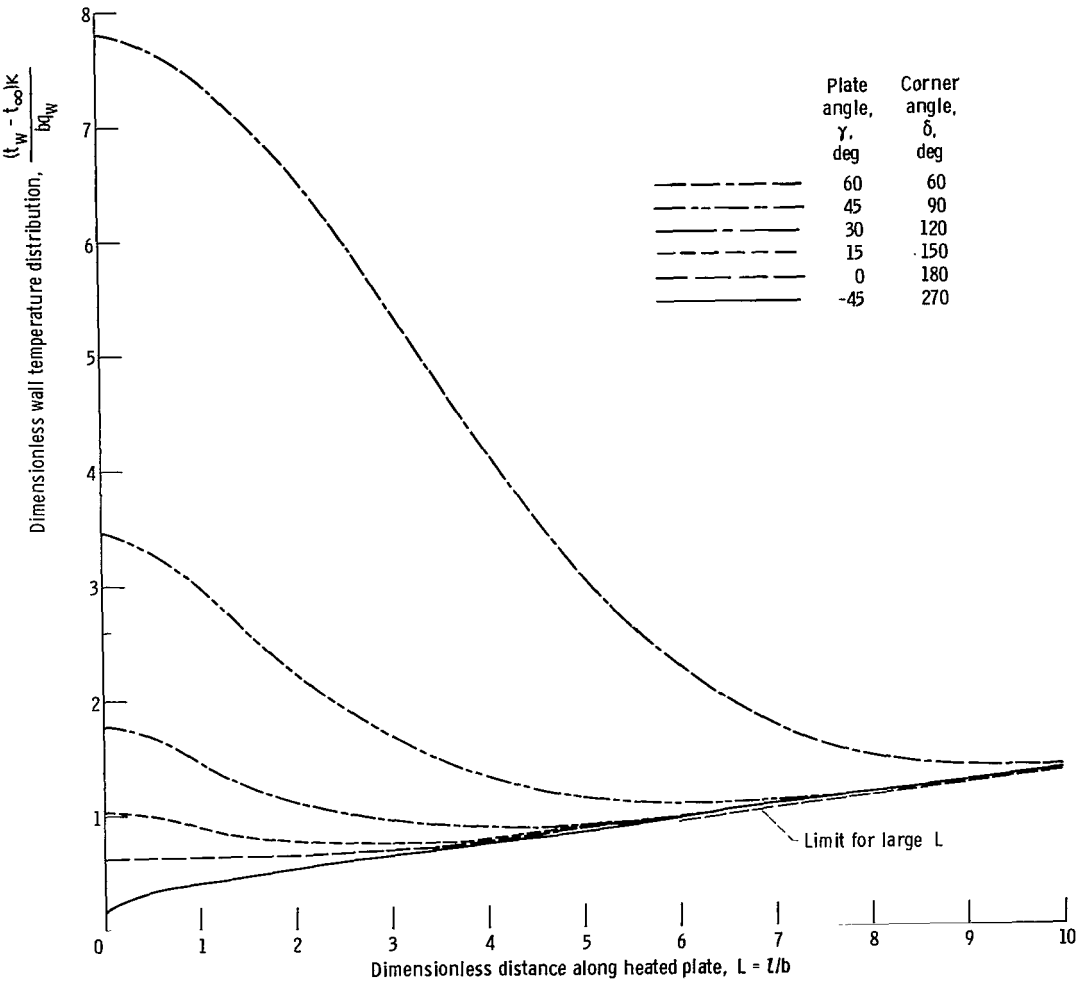

(c) Jet Péclet number, 20.

Figure 8 - Continued.

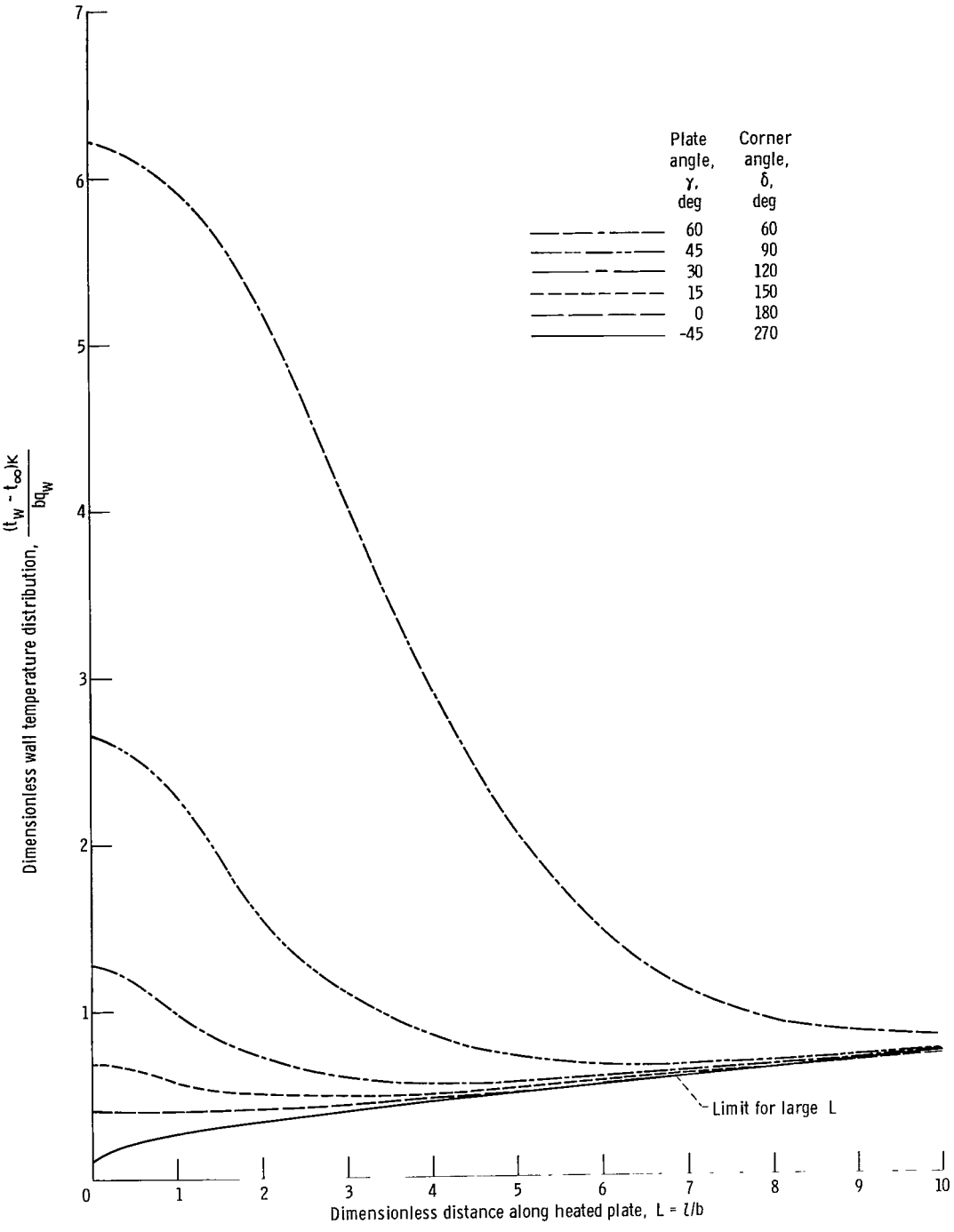

(d) Jet Péclet number, 50.

Figure 8. - Concluded.

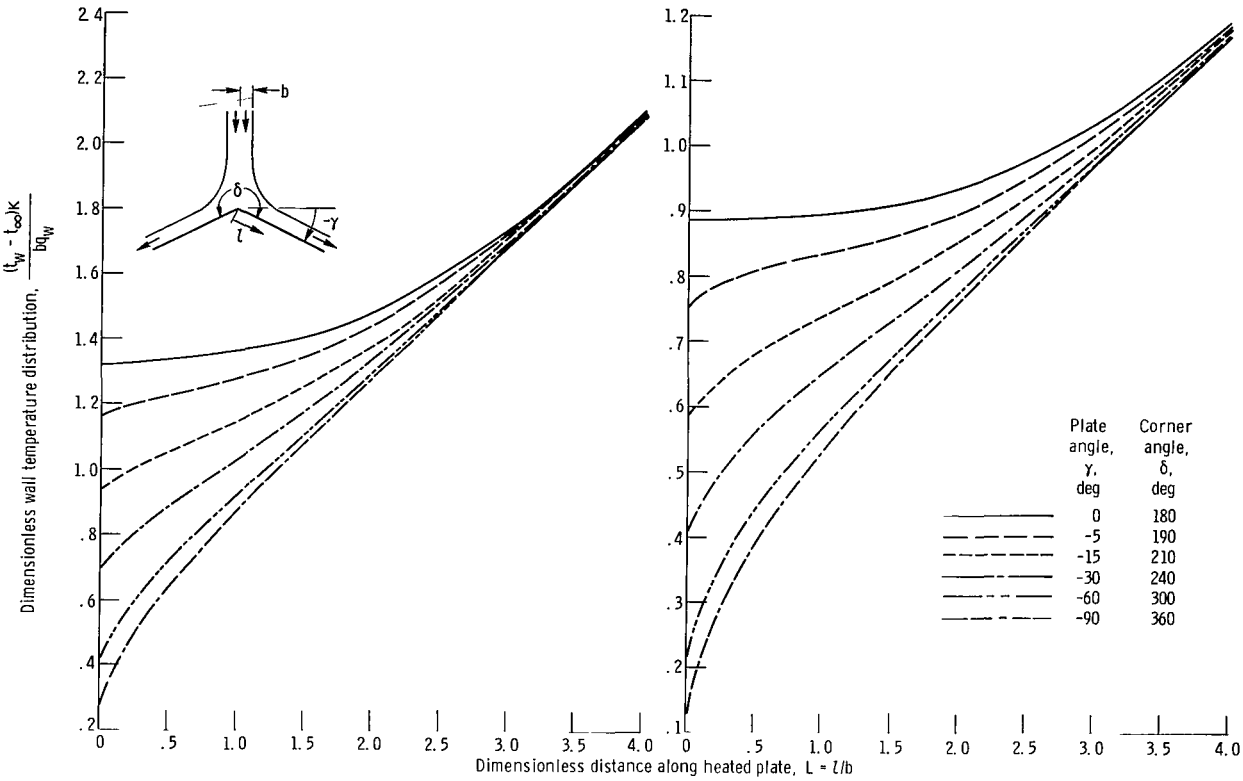

(a) Jet Péclet number, 5.

(b) Jet Péclet number, 10.

Figure 9. - Effect of angle of impingement plate on dimensionless wall temperature distribution for fixed value of jet Péclet number at plate angles from -90 to 0°.

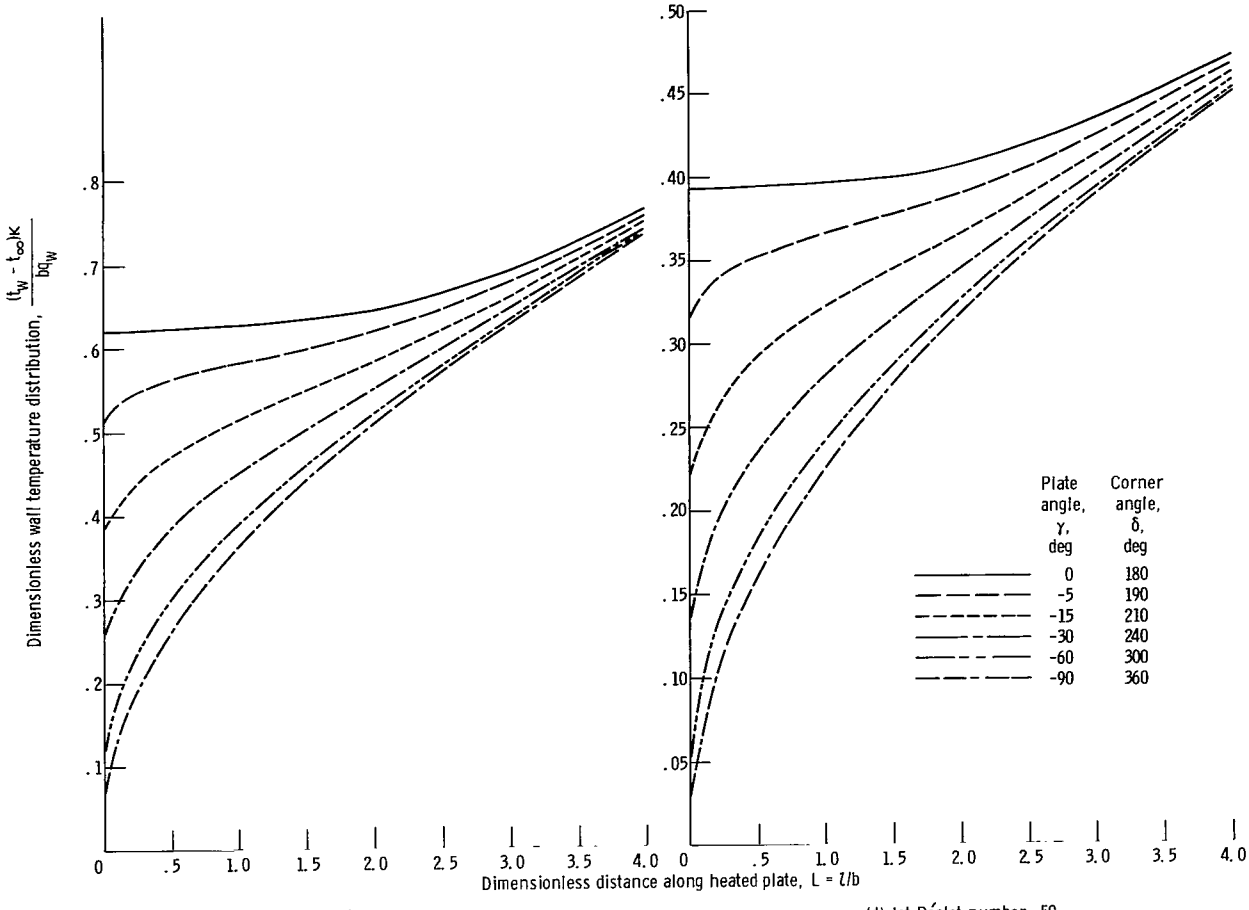

(c) Jet Péclet number, 20.

(d) Jet Péclet number, 50.

Figure 9. - Concluded.

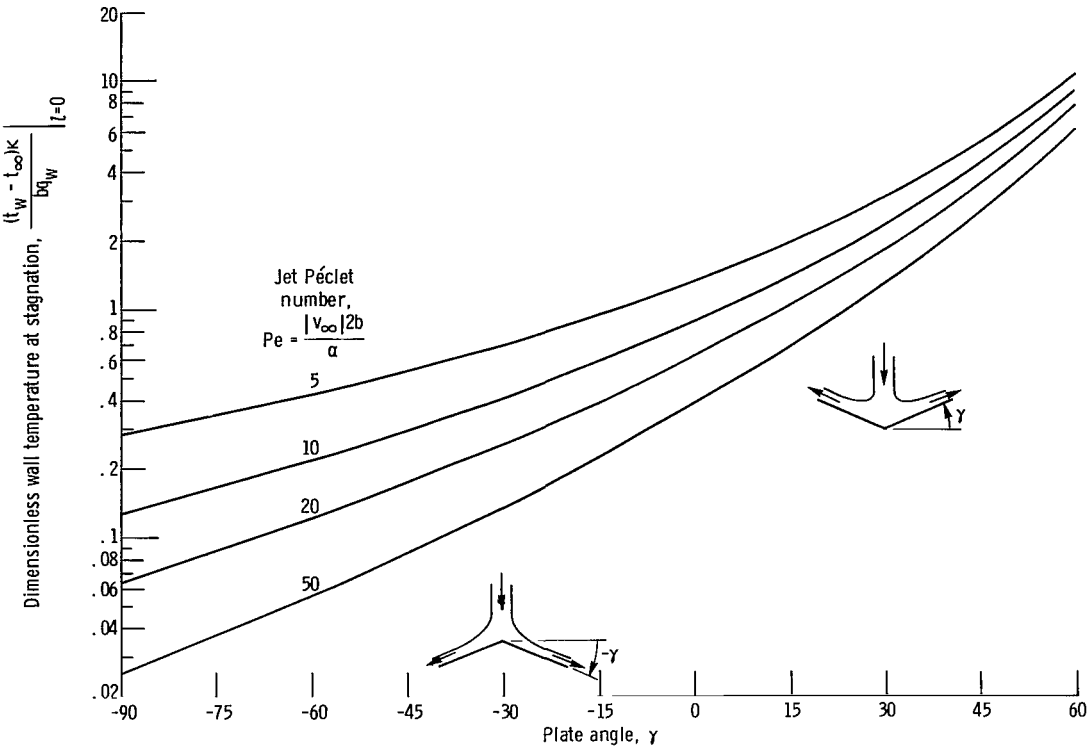

Figure 10. - Dimensionless wall temperatures at stagnation (apex of flat plates) as function of plate angle for various jet Péclet numbers.

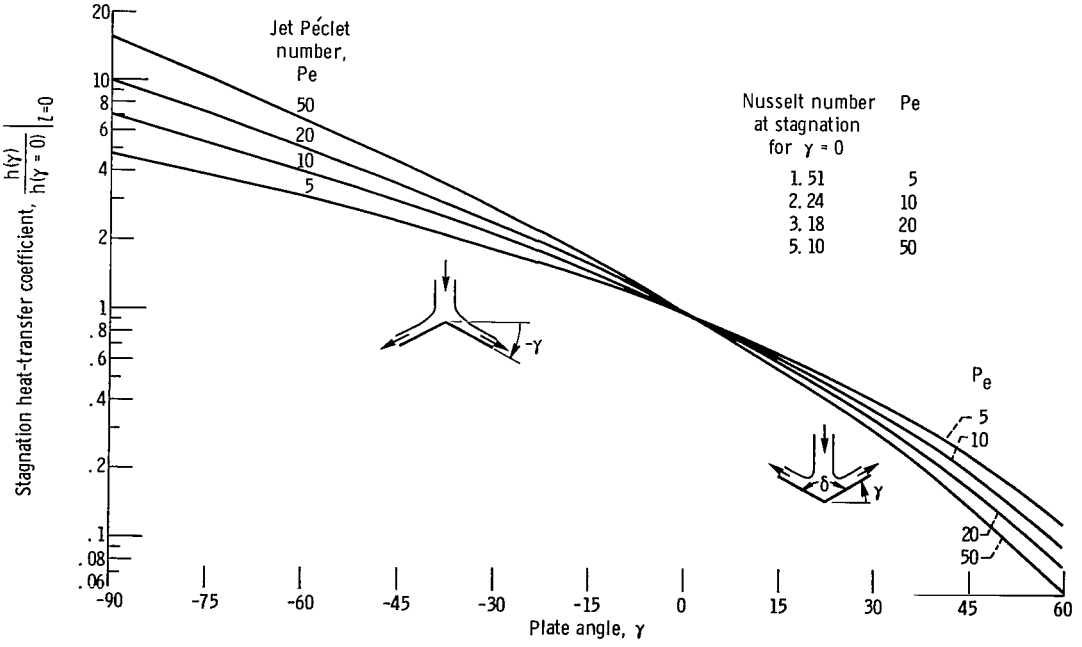

Figure 11. - Stagnation heat-transfer coefficient for plate at angle, relative to coefficient at stagnation point of flat plate.

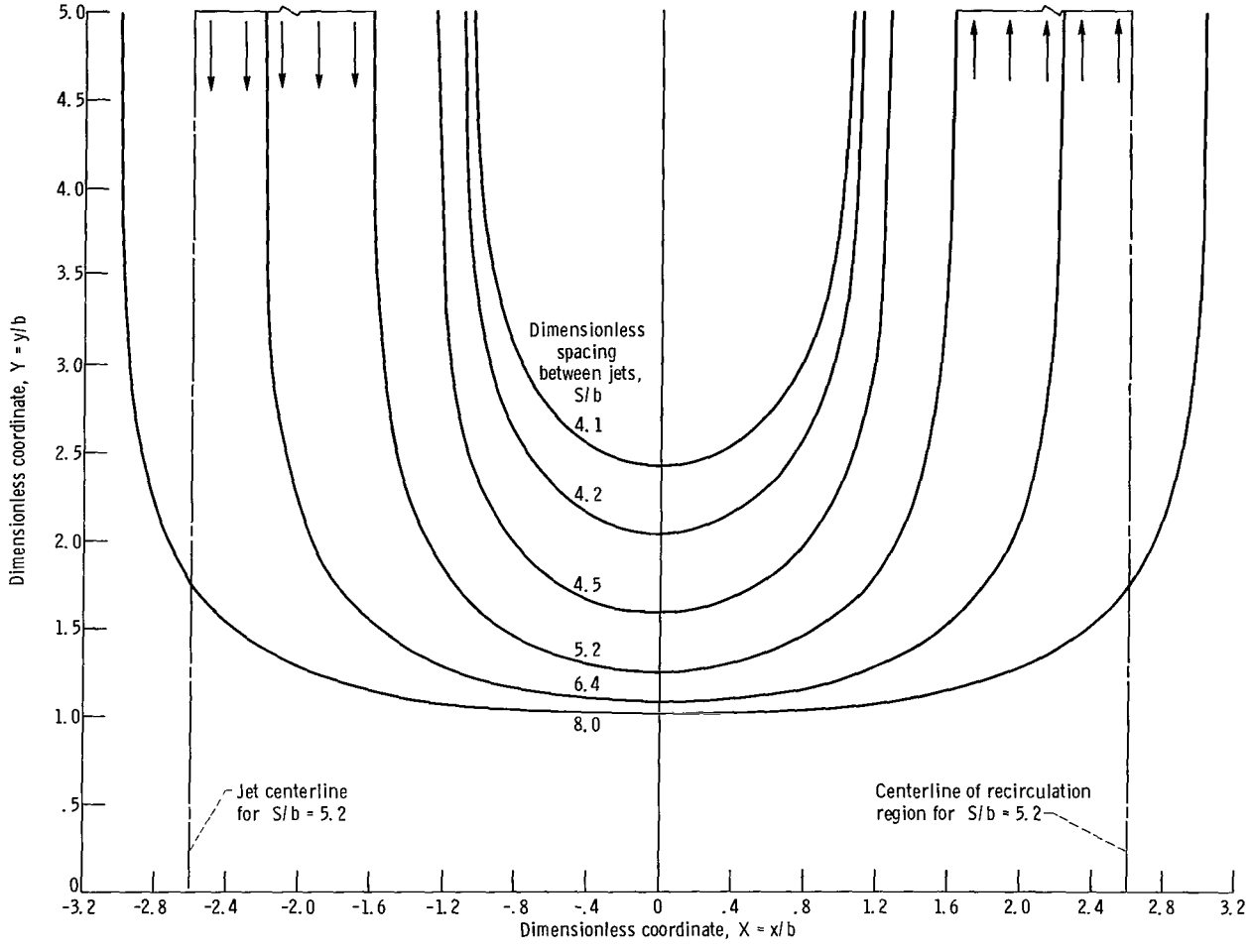

Figure 12. - Free streamlines for infinite row of jets impinging on flat plate for various spacing between jets.

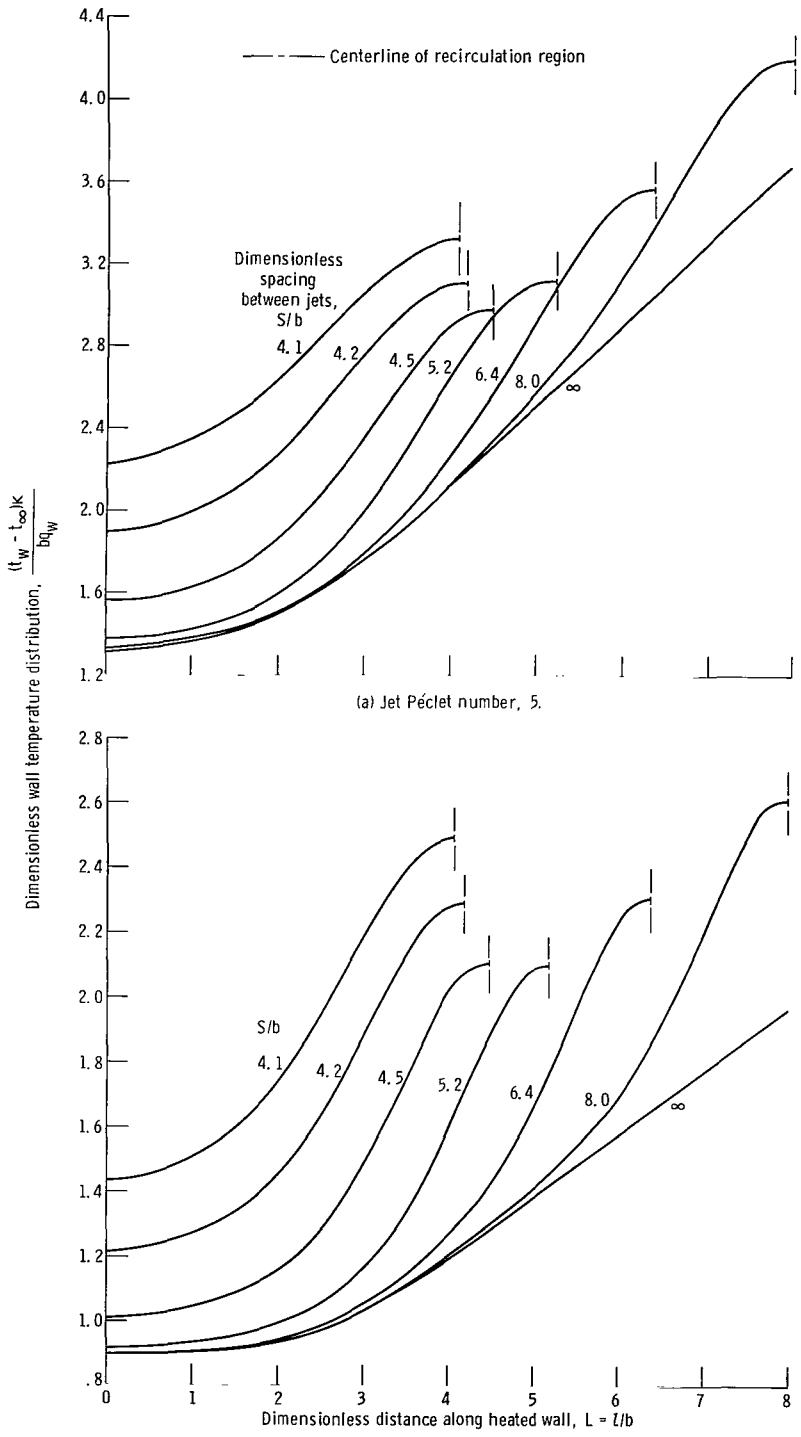

(a) Jet Péclet number, 5.

(b) Jet Péclet number, 10.

Figure 13. - Effect of spacing between jets on dimensionless temperature distribution along heated wall.

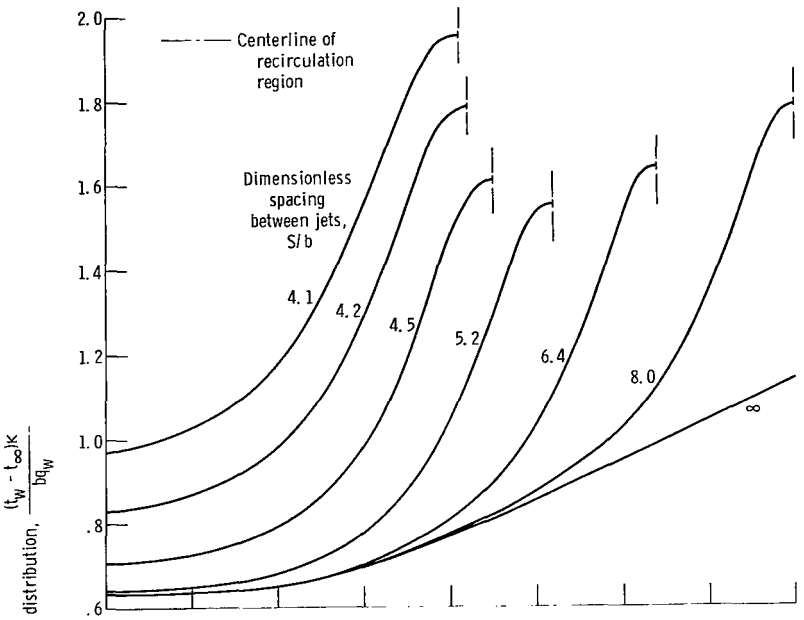

(c) Jet Péclet number, 20.

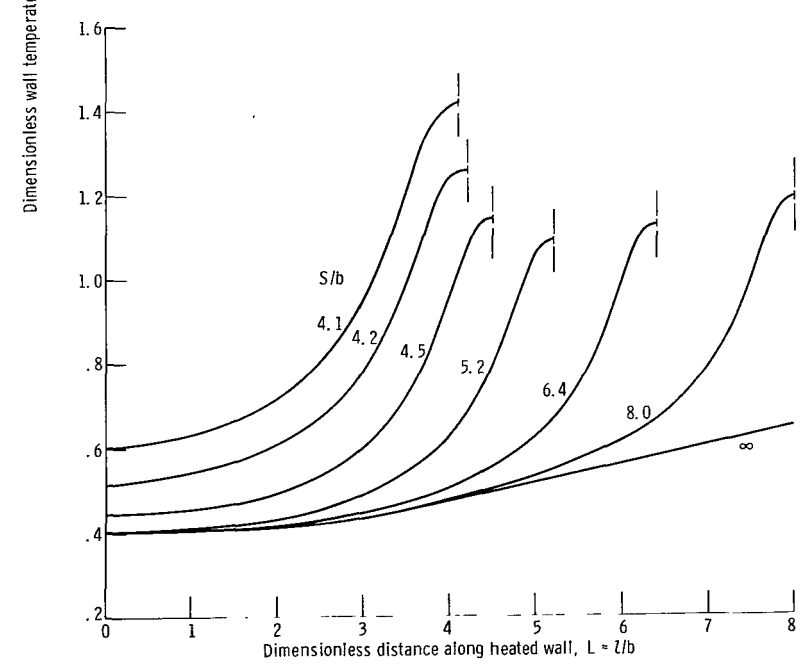

(d) Jet Péclet number, 50.

Figure 13. - Concluded.

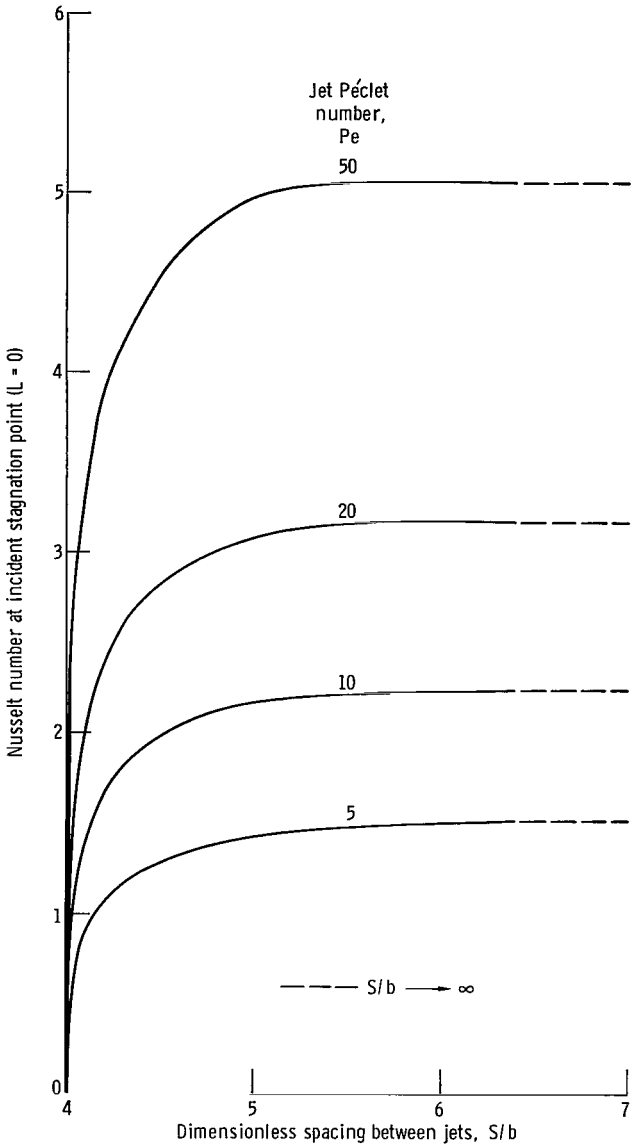

Figure 14. - Effect of jet spacing and Péclet number on Nusselt number at stagnation point of incident jet.

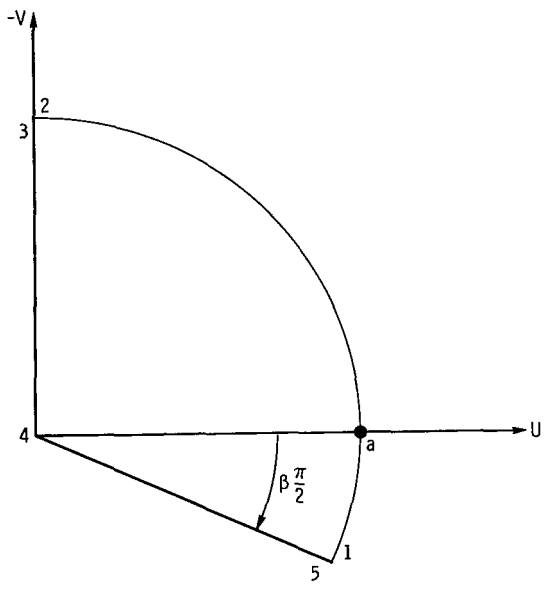

(a) Positive β.

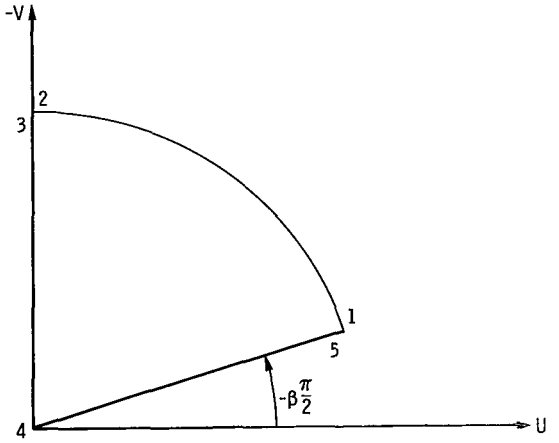

(b) Negative β.

Figure 15. - Dimensionless hodograph plane, $\zeta = U - iV$.

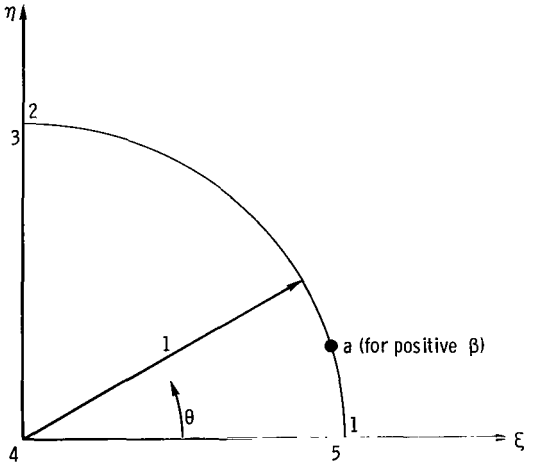

Figure 16. - Auxiliary t-plane, $t = \xi - i\eta$.

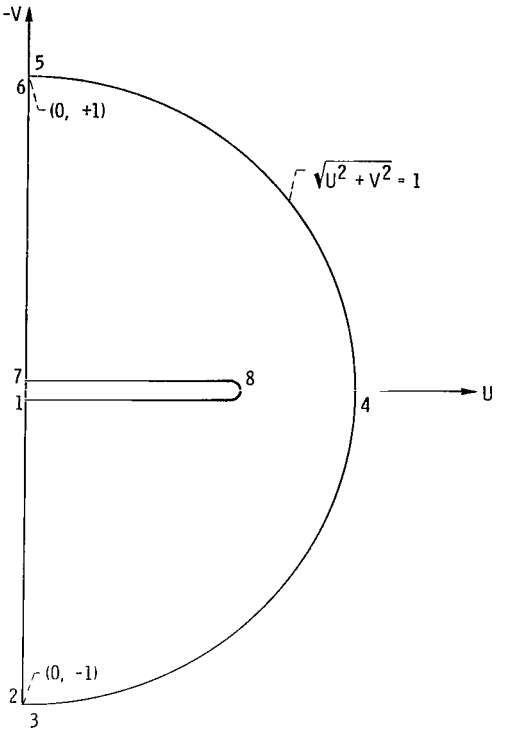

Figure 17. - Hodograph plane U - iV.

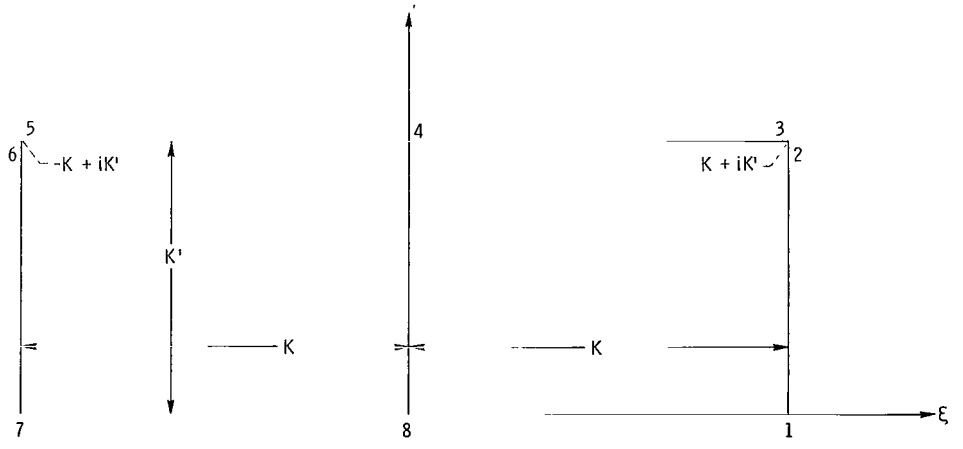

Figure 18. - Auxiliary u-plane.

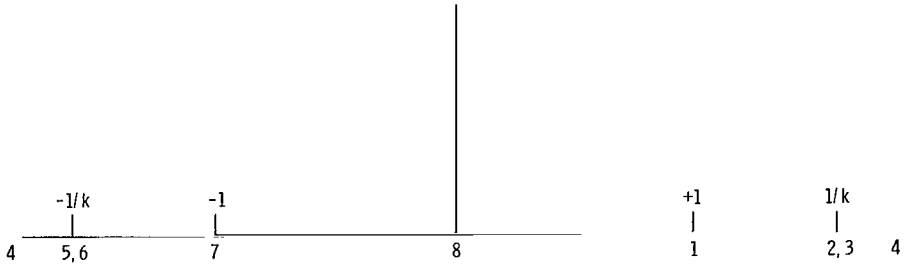

Figure 19. - Auxiliary T-plane.

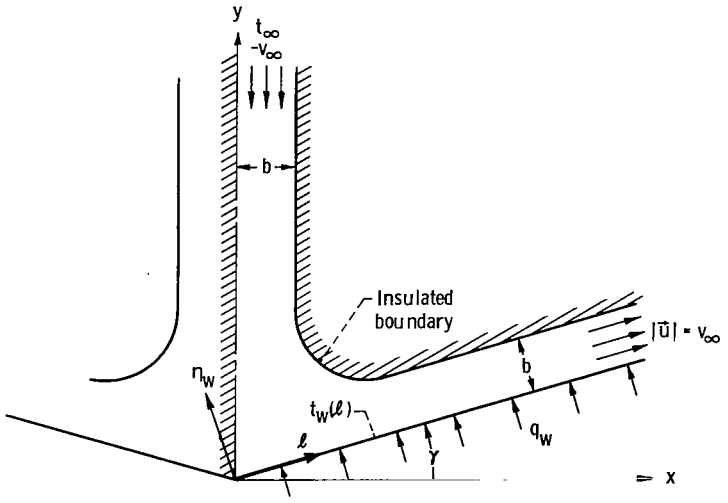

Figure 20. - Geometry for derivation of heat-transfer behavior at large ℓ.

"The aeronautical and space activities of the United States shall be conducted so as to contribute . . . to the expansion of human knowledge of phenomena in the atmosphere and space. The Administration shall provide for the widest practicable and appropriate dissemination of information concerning its activities and the results thereof."

—NATIONAL AERONAUTICS AND SPACE ACT OF 1958

NASA SCIENTIFIC AND TECHNICAL PUBLICATIONS

TECHNICAL REPORTS: Scientific and technical information considered important, complete, and a lasting contribution to existing knowledge.

TECHNICAL NOTES: Information less broad in scope but nevertheless of importance as a contribution to existing knowledge.

TECHNICAL MEMORANDUMS: Information receiving limited distribution because of preliminary data, security classification, or other reasons. Also includes conference proceedings with either limited or unlimited distribution.

CONTRACTOR REPORTS: Scientific and technical information generated under a NASA contract or grant and considered an important contribution to existing knowledge.

TECHNICAL TRANSLATIONS: Information published in a foreign language considered to merit NASA distribution in English.

SPECIAL PUBLICATIONS: Information derived from or of value to NASA activities. Publications include final reports of major projects, monographs, data compilations, handbooks, sourcebooks, and special bibliographies.

TECHNOLOGY UTILIZATION PUBLICATIONS: Information on technology used by NASA that may be of particular interest in commercial and other non-aerospace applications. Publications include Tech Briefs, Technology Utilization Reports and Technology Surveys.

Details on the availability of these publications may be obtained from:

SCIENTIFIC AND TECHNICAL INFORMATION OFFICE

NATIONAL AERONAUTICS AND SPACE ADMINISTRATION

Washington, D.C. 20546